Influence of Pleistocene climatic oscillations on the phylogeography and demographic history of endemic vulnerable trees (section *Magnolia*) of the Tropical Montane Cloud Forest in Mexico

Yessica Rico[1,2], M. Ángel León-Tapia[3], Marisol A. Zurita-Solís[1], Flor Rodríguez-Gómez[4], Suria Gisela Vásquez-Morales[5]

[1] Red de Diversidad Biológica del Occidente Mexicano, Instituto de Ecología, A.C., Pátzcuaro, Michoacán, Mexico.

[2] CONACyT, 03940, Ciudad de México, Mexico.

[3] Laboratorio de Sistemática Filogenética, Biología Evolutiva, Instituto de Ecología A.C., Xalapa, Veracruz, Mexico

[4] Departamento de Ciencias Computacionales, División de Electrónica y Computación, Centro Universitario de Ciencias Exactas e Ingenierías. Universidad de Guadalajara, Guadalajara, Jalisco, Mexico.

[5] Departamento de Biología, División de Ciencias Naturales y Exactas, Universidad de Guanajuato, Guanajuato, Mexico

Corresponding author:

Yessica Rico[1,2]

[1] Red de Diversidad Biológica del Occidente Mexicano, Instituto de Ecología, A.C., Pátzcuaro, Michoacán, Mexico.

[2] CONACyT, 03940, Ciudad de México, Mexico.

yessica.rico@inecol.mx

1 **Abstract**

3 The Tropical Montane Cloud Forest (TMCF) is a highly dynamic ecosystem that has undergone
4 frequent spatial changes in response to the interglacial-glacial cycles of the Pleistocene. These
5 climatic fluctuations between cold and warm cycles have led to species range shifts and
6 contractions-expansions, resulting in complex patterns of genetic structure and lineage
7 divergence in forest tree species. In this study, we sequenced four regions of the chloroplast
8 DNA (*trnT-trnL, trnK5-matk*, *rpl32-trnL*, *trnS-trnG*) for 20 populations and 96 individuals to
9 evaluate the phylogeography, historical demography, and paleodistributions of vulnerable
10 endemic TMCF trees in Mexico: *Magnolia pedrazae* (north-region), *M. schiedeana* (central-
11 region), and *M. schiedeana* population Oaxaca (south-region). Our data recovered 49 haplotypes
12 that showed a significant phylogeographic structure in three regions: north, central, and south.
13 Bayesian Phylogeographic and Ecological Clustering (BPEC) analysis also supported the
14 divergence in three lineages and highlighted the role of environmental factors (temperature and
15 precipitation) in genetic differentiation. Our historical demography analyses revealed
16 demographic expansions predating the Last Interglacial (LIG, ~125,000 years ago), while
17 Approximate Bayesian Computation (ABC) simulations equally supported two contrasting
18 demographic scenarios. The BPEC and haplotype network analyses suggested that ancestral
19 haplotypes were geographically found in central Veracruz. Our paleodistributions modeling
20 showed evidence of range shifts and expansions-contractions from the LIG to the present, which
21 suggested the complex evolutionary dynamics associated to the climatic oscillations of the
22 Pleistocene. Habitat management of remnant forest fragments where large and genetically
23 diverse populations occur in the three TMCF regions analyzed would be key for the conservation
24 of these magnolia populations.

37 **Introduction**

39 Examining population genetic structure over historical spatial and temporal scales and its
40 relationship with environmental changes is crucial for understanding species distributions and
41 adaptations to the ongoing climatic changes (Scoble & Lowe, 2010; Dalmaris et al., 2015). This
42 information is extremely pertinent for vulnerable ecosystems of high species diversity and
43 endemism in tropical regions. In Mexico, the Tropical Montane Cloud Forest (TMCF) covers
44 less than 1% of the Mexican territory but has the highest biotic diversity per unit area that nearly
45 accounts for 10% of the flora (Rzedowsky, 1978; Rzedowsky, 1996) and 12% of the terrestrial
46 vertebrates at the national level (Pineda et al., 2005; Sánchez-González et al., 2008). The TMCF
47 usually occurs between 1200 to 2500 m.a.s.l., and with a patchy distribution in narrow strips
48 along mountainous ranges (Rzedowsky, 1978; Alcántara et al., 2002). This ecosystem harbors
49 highly specialized species dependent on microclimatic conditions associated to the presence of
50 fog, high atmospheric humidity, and frequent rainfall (1000 to 5000 mm) (Rzedowsky, 1978;
51 Cruz-Cárdenas et al., 2012), which implies that the TMCF is very vulnerable to climate change
52 (Ponce-Reyes et al., 2012).
53   The TMCF is a highly dynamic ecosystem, which has undergone frequent spatial changes
54 in response to physical and climatic phenomena over geological time scales since the Neogene
55 (Graham 1999; Rahbek et al. 2019), and with acute changes during the interglacial-glacial cycles
56 of the Quaternary (Ramírez-Barahona & Eguiarte, 2013; Guevara, 2020). During this period, the
57 climatic variations between cold and warm cycles resulted in expansions and contractions of the
58 TMCF due to the species dependency to the high atmospheric humidity (Ramírez-Barahona &
59 Eguiarte, 2013). These processes led to complex patterns of connectivity and fragmentation on
60 species distributions, evolutionary adaptations to local environmental conditions and lineage
61 divergence in plant and animal populations (Gutiérrez-Rodríguez et al., 2011; Ornelas et al.,
62 2013; Venkatraman, 2019; Rahbek et al., 2019). Species demographic dynamics of the TMCF in
63 response to the climatic oscillations of the Pleistocene in the Neotropics have been explained by
64 two main precipitation models (reviewed in Ramírez-Barahona & Eguiarte, 2013). The dry
65 refugia model states that the cool conditions during the Last Glacial Maximum (LGM ~23 ka)
66 led to downslope migrations but the arid conditions in the lowlands resulted in species range
67 contractions into glacial refugia. Subsequently in the Holocene (~11.7- 8.3 ka) with the increase
68 in temperature and humidity, populations expanded and re-colonized their former distribution
69 ranges (Prance 1982; Ramírez-Barahona & Eguiarte, 2013). According to the dry refugia and
70 based on the distribution of endemic species and centers of endemism, Toledo (1982) postulated
71 eight glacial refugia for forest species in Mexico: five adjacent to Central America and three in
72 the drainage basin of the Gulf of Mexico in Veracruz and Oaxaca. Contrary to this model, the
73 moist forests model states that the prevalence of humid conditions during the LGM lead to
74 species migrations and expansions in the lowlands resulting in gene flow and wide range
75 population connectivity. Later during the Holocene, the increase in temperature would have led
76 to species range fragmentations and contractions into high altitude regions (Ramírez-Barahona &

77   Eguiarte, 2013). Each model would have led to different genetic signatures that can be contrasted
78   through analyses of phylogeography, demography, and ecological niche modeling (Ramírez-
79   Barahona & Eguiarte, 2013; Ornelas et al., 2019).
80   The most relevant genetic signatures according to the dry refugia are the genetic
81   differentiation of populations from separate refugia due to limited gene flow during the LGM, a
82   star-shaped allele genealogy of post-glacial expanding lineages and thus evidence of
83   demographic expansions. Decline of genetic diversity away from refugial regions might also be
84   expected by the occurrence of founder effects, whereas rare alleles would occur in high
85   frequency in refugial populations (Excoffier et al., 2009; Gutiérrez-Rodríguez et al., 2011;
86   Ramírez-Barahona & Eguiarte, 2013). For the moist forests model, the stability of humid
87   conditions during the LGM, which increased population connectivity, would have led to the
88   maintenance of genetic diversity and homogenization of genetic variation with no clear
89   geographical structuring (Twyford et al., 2012; Ramírez-Barahona & Eguiarte, 2013).
90   Demographic expansions and bottlenecks would be less likely to occur in large and continuous
91   populations. Genetic evidence shows mixed support for both models (see Ramírez-Barahona &
92   Eguiarte, 2013) and for alternative hypotheses (see Ornelas et al., 2019; Salces-Castellano et al.,
93   2021) in TMCF plant and animal species. Thus, gathering more data from other relevant endemic
94   species is needed to better understand the complex dynamics on the evolution of the TMCF.
95   Trees are good models to evaluate demographic and phylogeographic patterns due to
96   their long generation times that more likely preserve historical demographic signals. Moreover,
97   they provide foundational habitat for many specialized endemic flora and fauna, being key
98   elements of the TMCF biodiversity. Magnoliaceae is an ancient family of flowering trees and
99   shrubs (subfamily divergence ~78 - 47 Mya between the Cretaceous and the Eocene; Ramírez-
100   Barahona et al., 2020) that had a continuous distribution in North America and Asia in the
101   Eocene climatic optimum consistent with the Boreotropical flora (Dong et al., 2021). During the
102   Neogene, magnolias migrated southward to warmer and wetter conditions in high valleys and
103   mountain belts in Mexico, Central and South America (Hebda & Irving, 2004). In Mexico,
104   magnolias diversified with approximately 40 recognized species occurring in humid forests, such
105   as the TMCF and other ecosystems (Vázquez-García et al., 2017). Fossil records of *Magnolia*
106   seeds suggest they were abundant and widespread in the Northern Hemisphere in the Tertiary
107   (Azuma et al., 2001), but currently many species are geographically restricted and with small
108   population sizes (Rivers et al., 2016).
109   A representative magnolia species of the TMCF is *Magnolia schiedeana* Schltl., a narrow
110   endemic from the late Miocene (~10 Mya; Dong et al., 2021) occurring in the largest strip of the
111   TMCF in the Sierra Madre Oriental from Hidalgo to central Veracruz (Vázquez-García, 1994)
112   (Fig 1A). Due to its declining populations by anthropogenic threats of the TMCF, the species is
113   listed as endangered in the IUCN The Red List of Mexican Cloud Forest Trees (González-
114   Espinosa et al., 2011), as vulnerable by IUCN The Red List of Magnoliaceae (Rivers et al.,
115   2016) and protected under Mexico´s domestic legislation (NOM-059, SEMARNAT 2010).
116   *Magnolia schiedeana* was formerly considered to have a wider distribution, which included a

117 northern-limit distribution in San Luis Potosí and Querétaro, and two disjoint distributions in
118 eastern Guerrero and the Sierra de Juárez in northern Oaxaca (Vázquez-García, 1994).
119 Taxonomic studies based on morphological characters showed that specimens in these regions
120 were at least five different species (Guerrero: *M. vazquezii* Jiménez-Ramírez et al., 2007; *M.*
121 *guerrerensis*; Cruz-Durán et al., 2008; Oaxaca: *M. oaxacensis;* Vázquez-García et al., 2012; *M.*
122 *zamudioi;* Vázquez-García et al., 2013, and San Luis Potosí and Querétaro: *M. pedrazae;*
123 Vázquez-García et al., 2013), but for some populations in Oaxaca (Metates in Santiago
124 Comaltepec) the taxonomic identity remains unclear (A. Vázquez-García pers. comm.). Given
125 their patchy distribution along mountainous ranges, vicariance has been hypothesized as an
126 important mechanism in the evolution of many Mexican *Magnolia* (Vázquez, 1994). Despite that
127 the TMCF harbors a considerable number of magnolia species that are threatened by habitat loss
128 in Mexico (Vázquez-García et al., 2017; Rivers et al., 2016), the information about their
129 population genetics and demographic dynamics associated to the climatic changes of the
130 Pleistocene is almost lacking; this knowledge would shed light on the potential vulnerability of
131 *Magnolia* trees to climate change from an historical perspective (D'Amen et al., 2013).
132   In this study we analyzed 20 populations and 96 individuals of *M. pedrazae* and *M.*
133 *schiedeana* across their distribution in the Sierra Madre Oriental from San Luis Potosí to
134 Veracruz, and one population in Santiago Comaltepec Oaxaca, which here we denote as *M.*
135 *schiedeana* pop. Oaxaca. The distributions of these magnolia populations are within the largest
136 strip of TMCF at the east of Mexico, which here we distinguish in three regions: north (*M.*
137 *pedrazae*), central (*M. schiedeana*), and south (*M. schiedeana* pop. Oaxaca) (Fig. 1).
138 Specifically, by sequencing four chloroplast DNA regions (*trnT-trnL, trnK5-matk, rpl32-trnL,*
139 *trnS-trnG*) our aims were to: (*i*) perform a phylogeographic approach to evaluate the historical
140 signatures of the genetic divergence between *M. pedrazae*, *M. schiedeana* and *M. schiedeana*
141 pop. Oaxaca, and (*ii*) evaluate whether demographic changes and past species distributions were
142 influenced by the climatic oscillations of the Pleistocene.
143
144 **Material and methods**
145
146 *Study species*
147
148 *Magnolia schiedeana* is a perennial tree (> 200 years) up to 25 meters in height (Rodríguez-
149 Ramírez et al., 2020). The species flowers from April to June, has sexual reproduction but can
150 reproduce clonally by sprouting from the base of the trunk (Vásquez-Morales et al., 2017). Seed
151 dispersal occurs by birds and small mammals (Watanabe et al., 2002) and pollination by a
152 specialist beetle *Cyclocephala jalapensis* (Dieringer & Espinosa, 1994). *Magnolia pedrazae*
153 occurs in remnant TMCF fragments in the north of Querétaro and southeast San Luis Potosí,
154 whereas nothing is known about its biology. This species is listed as endangered by the IUCN
155 Red List (Rivers et al., 2016), but not included under the Mexican domestic legislation.
156

157   *Sampling and DNA sequencing*

158

159   During February to November 2019, we collected leaf tissue samples from 15 remnant *M.*
160   *schiedeana* populations from the states of Hidalgo, Puebla, and Veracruz. Moreover, we
161   collected individuals from one locality in Santiago Comaltepec in Oaxaca, where its taxonomic
162   identity is unclear. Additionally, we included four populations from *M. pedrazae* in Querétaro
163   and San Luis Potosí, which samples were collected in a previous study in 2017 (Rico &
164   Gutiérrez-Becerril, 2019) for a total of 20 populations (Table 1, Fig. 1). We randomly collected
165   young leaf samples from up to 10 adults or juvenile's trees and with a minimum separation
166   between sampled trees of 10 m. Leaves were preserved in sealable plastic bags containing silica
167   gel until DNA extractions were performed. GPS coordinates were recorded for each locality.
168   Permission to conduct our fieldwork was granted by the Mexican government (SEMARNAT
169   SGPA/DGGFS/712/1062/18).
170   Genomic DNA from 20 mg of dried tissue was extracted following the CTAB extraction
171   protocol of Doyle & Doyle (1987). We amplified four chloroplast (cpDNA) intergenic spacers:
172   *trnT-trnL* (744 bp), *trnK5-matk* (789 bp), *rpl32-trnL* (624 bp) (Azuma et al., 2011), and *trnS-*
173   *trnG* (702 bp) (Shaw et al., 2005). PCR reactions were carried out using the MyTaq™ DNA
174   polymerase kit (BIOLINE, London, United Kingdom) following the conditions outlined in Rico
175   & Gutiérrez-Becerril (2019). Using the forward primers, PCR products were sequenced in
176   MAGROGEN Inc. (Seoul, South Korea). A positive and negative control were included in each
177   PCR plate to control for contamination. The quality of sequences was revised and edited in
178   CHROMAS v2.6.5 (Technelysium Pty Ltd). We successfully sequenced 85 individuals, which
179   unique sequences are available in NCBI GENBANK (www.ncbi.nlm.nih.gov) (NCBI accession
180   numbers *trnK5-matk*: MW321790-321798, *rpl32-trnL*: MW321799-MW321808, *trnS-trnG:*
181   MW321809-MW321812, *trnT-trnL*: MW321813- MW321827). Additionally, we used four
182   cpDNA sequences from eight *M. pedrazae* individuals from San Luis Potosí and Querétaro and
183   three *M. schiedeana* from Veracruz (CP population) obtained from Rico & Gutiérrez-Becerril
184   (2019) for a total of 96 individuals.

185

186   *Phylogenetic and haplotype relationships*

187

188   Sequences were aligned using MUSCLE v3.8.31 algorithm (Edgar, 2004) with default
189   parameters and subsequently manually adjusted in MEGA X (Kumar et al., 2018). To reconstruct
190   phylogenetic relationships, we included sequences from other *Magnolia* species available from
191   GENBANK: *Liriodendron chinese* (KU170538), *M. mexicana,* Section Talauma (MN700657),
192   *M. ovata* Section Talauma (MT293605), *M. tripetala* Section Rhytidospermum (AY727271,
193   DQ826283, AY727517), *M. acuminata* Section Tulipastrum (MN990595), *M. virginiana* Section
194   Magnolia (AB553858, AB553841, AB553861, AB553852), *M. iltisiana* Section Magnolia
195   (MK210435, MK210442, MK210448, MK210453), and one sequence obtained in this study
196   from *M. pacifica* Section Magnolia (Locality San Sebastián del Oeste, Jalisco). These species

197   were chosen based on their closely phylogenetic relationships and *L. chinese* as the sister group
198   of *Magnolia* (Azuma et al., 2011; Wang et al., 2020). The sequence from *L. chinese* was used as
199   outgroup to root the tree. The four cpDNA sequences were concatenated using
200   SEQUENCEMATRIX (Vaidya et al., 2011). The best substitution model fitting each marker was
201   selected using the Akaike information criterion (AIC) in JMODELTEST v2.1.10 (Darriba et al.,
202   2012). A consensus phylogenetic tree was obtained by Bayesian Inference (BI) using
203   MRBAYES v3.2.2 (Huelsenbeck & Ronquist, 2001), by performing two independent runs of
204   three cold chains, one heated chain, and specifying 20,000,000 generations with sampled trees
205   every 1,000 generations. We assessed convergence until we reached an average standard
206   deviation of split frequencies below 0.01. We discarded the first 25% of generated trees as burn-
207   in, and posterior probabilities (PP) were estimated from the posterior distribution of retained
208   trees.
209   Genealogic relationships were obtained by constructing a median-joining (MJ) haplotype
210   network in POPART (Leigh & Bryant, 2015) for the concatenated cpDNA matrix of *M.*
211   *pedrazae* (n = 17), *M. schiedeana* (n = 74) and *M. schiedeana* pop. Oaxaca (n = 5). All
212   subsequent analyses were carried for this 96 individual's data set.
213
214   *Genetic diversity, differentiation, and phylogeographical structure*
215
216   For each sampled locality and for the three lineages, we estimated the mean haplotype (*Hd*) and
217   nucleotide diversity (π) using DNASP v6.12.03 (Rozas et al., 2017). Analyses of molecular
218   variance (AMOVA) were performed to evaluate the amount of genetic variance and genetic
219   differentiation (F_{ST}) found in the following groupings: (1) no predefined groups, (2) populations
220   in two lineages, *M. pedrazae* + *M. schiedeana* and *M. schiedeana* pop. Oaxaca, and (3)
221   populations in three lineages, *M. pedrazae*, *M. schiedeana* and *M. schiedeana* pop. Oaxaca.
222   AMOVAs were performed using the Tamura and Nei genetic distance and with 1000
223   permutations to determine the statistical significance of each partition as implemented in
224   ARLEQUIN v3.5.2.2 (Excoffier & Lischer, 2010). Evidence of phylogeographic structure was
225   determined by contrasting the coefficients of population differentiation G_{ST} and N_{ST}. A
226   significantly higher N_{ST} than G_{ST} is evidence of a significant phylogeographical structure
227   resulting from the occurrence of closely related haplotypes in populations (Pons & Petit, 1996).
228   These coefficients were obtained using PERMUT v2.0 (Pons & Petit, 1996) with 10,000
229   permutations.
230   We used BAPS v5.3 (Corander et al., 2008) to determine the most likely number of
231   genetic clusters using the clustering of linked loci module and the codon linkage model,
232   appropriate for sequence data. First, with few replicates (n = 5) and three independent runs, we
233   explored the likely number of genetic clusters from *K* = 2 to 10. By looking at the posterior
234   probabilities and likelihood values, we observed that the most likely number of clusters was
235   between 3 and 5 and thus the final analysis was carried out with two independent runs for *K* = 2
236   to 5 with 10 replicates each. The most likely number of *K* clusters was determined by its higher

237 posterior probability and likelihood value. Additionally, pairwise F_{ST} comparisons were
238 calculated in ARLEQUIN v3.5.2.2 with 1000 permutations to test for statistically significant
239 differences between lineages. Mantel correlations to test the effect of isolation by geographical
240 distance (IBD) on G_{ST} genetic and Euclidean distances was examined for the overall data set.
241 Significance of the Mantel correlation was tested by permuting observations 1,000 times using
242 the R library vegan 2.5.7 (Oksanen et al., 2015) (R core Team, 2020).
243
244 *Environmental differentiation on phylogeographic genetic clusters*
245
246 We implemented a Bayesian Phylogeographic and Ecological Clustering analysis (BPEC) in the
247 BPEC v1.3.1 R package to reveal the geographical distribution of genetic clusters by considering
248 genetic, geographical, and environmental data (Manolopoulou et al., 2011; Manolopoulou and
249 Emerson 2012). This analysis assumes that population substructure is the result of migration
250 events into new sites, which can be explained by geographical and ecological restrictions to gene
251 flow (Manolopoulou et al., 2020). The test also provides measures of uncertainties for haplotype
252 relationships and identify likely ancestral locations (Manolopoulou et al., 2020). We analyzed all
253 cpDNA haplotypes, geographical locations, and current bioclimatic data extracted for each
254 individual occurrence for 19 bioclimatic layers in 30 arc-seconds (Karger et al., 2017)
255 downloaded from CHELSA (https://chelsa-climate.org).We discarded correlated bioclimatic
256 variables ($r \geq 0.8$, see ecological niche modeling) and use the first two synthetic axes from
257 Principal Components Analysis (PCA) as covariates. After several initial short runs, the final
258 analysis was carried out with two maximum number of migrations and relaxation of the
259 parsimony criterion not allowed (zero) to reach convergence. MCMC chains were run for 10
260 million steps with 10,000 posterior samples saved.
261   Additionally, statistical differences in the environmental space occupied for each lineage
262 was tested on the two PC axes with a Multivariate Analysis of Variance (MANOVA) using the
263 Pillai's trace as the test statistic (Nakazato et al., 2020). Moreover, we performed post hoc
264 Tukey-HSD pairwise comparisons on each of the PC axes (Di Febbraro et al., 2017) using the
265 base packages in R.
266
267 *Historical demography*
268
269 To infer historical demographic changes, we used different methods. First, we estimated
270 neutrality tests, Tajima's D (Tajima, 1989), Fu´s F (Fu, 1997), and *R2* (Ramos-Onsins & Rozas,
271 2002) with 1000 permutations using PEGAS R package (Paradis, 2010). Significant negative
272 values of Tajima's D and Fu´s F and positive *R2* values suggest rejection from neutrality and can
273 be interpreted as population expansion. Second, we computed pairwise nucleotide mismatch
274 distributions to contrast observed and expected distributions under a demographic growth-
275 decline model using DNASP v6.12.03 (Rozas et al., 2017). A unimodal pairwise distribution is
276 expected under a demographic expansion model, whereas a multimodal distribution would be

277   expected for populations at demographic equilibrium (Harpending et al., 1998). Mismatch
278   distributions were tested with the sum of square deviations (SSD) and the Harpending's
279   raggedness index (Hri) by implementing 1000 permutations in ARLEQUIN v3.5.2.2 (Excoffier
280   & Lischer, 2010). Significant SSD and Hri values ($P \leq 0.05$) indicate deviations from the sudden
281   expansion model. Third, we used Bayesian skyline plots in BEAST v2.4.2 (Drummond &
282   Bouckaert, 2015) to assess effective population size (Ne) changes across time. Two independent
283   analyses were run, one for *M. schiedeana* (n = 74) and one for *M. pedrazae* (n = 17). We used
284   the substitution model GTR+I as selected using AIC in JMODELTEST v2.1.10 (Darriba et al.,
285   2012). Other parameters used were empirical base frequencies, a relaxed clock lognormal model,
286   one run of 20 million generations, and trees and parameters sampled every 2000 iterations. The
287   time axis was scaled with the substitution rates 1.59×10^{-9} for chloroplast-wide, synonymous
288   substitution rates described for most angiosperms (Wolfe et al., 1987). After the analysis, we
289   viewed the log file in TRACER v1.7.1 (Rambaut et al., 2018) to ensure that effective sample
290   sizes (ESS) for all priors were > 200 (Drummond & Bouckaert, 2015). The mismatch
291   distribution plot and the Bayesian Skyline for *M. schiedeana* pop. Oaxaca was not possible due
292   to small sample size.
293   Lastly, we used an Approximate Bayesian Computation (ABC) framework implemented
294   in DIYABC v2.1 (Cornuet et al., 2008, 2014) to test for distinct competing demographic
295   scenarios. According to the results of BAPS and BPEC, we contrasted five likely scenarios. At
296   generation t_0 (present), all scenarios had the three genetic lineages. The first scenario predicts
297   that the three lineages diverge at the same time from a common ancestor (Na) at time t_2 and
298   remained without demographic changes until time t_0 (stable model). Scenarios 2, 3, and 4, predict
299   divergence at time t_1 between two of the lineages to subsequently merge the three lineages at
300   time t_2 (divergence model). The difference between these three scenarios is the lineage diverging
301   at time t_2, and subsequently the pair of lineages diverging at time t_1 (see results). Lastly, the fifth
302   scenario predicts a split between *M. schiedeana* and *M. schiedeana* pop. Oaxaca at time t_2, then
303   both lineages merge with *M. pedrazae* at time t_1 (admixture model). We considered these five
304   scenarios as the most plausible given the observed relationships of divergence and admixture
305   among the three lineages. Prior to the final run, we performed six runs to compare different
306   parameter conditions. The run that we present in the results (see below) was the run with best
307   adjusted parameters (Supplemental material). Each run was implemented with 2 million
308   coalescent-based simulated datasets and different summary statistics.
309   For the final run and given the absence of information on the species population sizes, we
310   used default priors. We generated three million coalescent-based simulated datasets for each of the
311   five evolutionary scenarios considering the HKY model, and *Na, N1, N2* and *N3* with a uniform
312   prior distribution with a minimum of 10 and a maximum of 100,000 values for effective population
313   sizes; the prior distribution of the timing of events was for t_1 and t_2 100 -100 000 generations
314   respectively and considering a 10-year generation time (Vazquez-Morales & Sánchez-Vélasquez,
315   2011). The set condition ($t_2 \geq t_1$) on the prior time distribution was added up to avoid
316   incongruences in the simulated genealogies. For the final run, we used the following summary

317   statistics: (1) For the three groups: Number of segregating sites, mean pairwise differences, and
318   mean number of the rarest nucleotide at segregation sites; (2) For the 1-2, 1-3 and 2-3 groups:
319   Number of segregating sites and F_{ST}. We used a prior distribution of mean mutation rates of 1.59 ×
320   10^{-9} for the chloroplast (Wolfe et al. 1987). We used the default parameters for the mutation model
321   section. Scenario posterior probabilities were evaluated using a logistic regression on the 1% of
322   simulated datasets nearest to the observed data (Fontaine et al., 2013). For the best-supported
323   scenario, we performed a model checking procedure by applying a PCA on test statistic vectors to
324   visualize the fit between the observed and simulated datasets. Confidence of the scenario choice
325   was assessed by simulating 500 pseudo-observed datasets (PODs) under each scenario to calculate
326   Type I and II error rates. Finally, for the best-supported scenario, we obtained point estimates for
327   demographic and temporal parameters using local linear regression on the 1% of simulations
328   nearest to the observed dataset (Cornuet et al., 2008, 2014).
329
330   *Present and past distribution ecological niche modeling*
331
332   Due to the taxonomic uncertainty for *Magnolia* species, we only used the occurrences from
333   specimens of *M. schiedeana*, *M. pedrazae*, and samples from Oaxaca collected in this study
334   (Supplemental Table S1). We used these occurrences because they have the quality and spatial
335   accuracy to produce models with ecological plausibility (Galante et al., 2018). To avoid sampling
336   biases, the occurrences were spatially thinned at three kilometers as a larger radius would have
337   significantly reduce the final number of occurrences; this was carried in the SPTHIN v0.1.0.1 R
338   package (Aiello-Lammens et al., 2015). Additionally, a second data set was built with occurrences
339   downloaded from the Global Biodiversity Information Facility (GBIF; http://www.gbif.org/), but
340   due to the likely uncertainty of some of these records, we also included localities reported in
341   previous studies, such as herbaria specimens of *M. schiedeana* (Vásquez-Morales et al., 2014,
342   2017). Specimens with insufficient locality information were discarded; all occurrences were
343   thinned at five kilometers due to a higher density of occurrences than the training data set. The first
344   data set included 26 occurrences used for building the niche model and the second data set
345   included 50 occurrences used for testing the models. As variable predictors, we used the 19
346   bioclimatic layers in 30 arc-seconds from CHELSA because these layers have a better performance
347   than other layers commonly used and can increase the accuracy of species range predictions
348   (Karger et al. 2017). The environmental layers were delimited to several polygons of the level II
349   ecoregions of North America downloaded from the United States Environmental Protection
350   Agency (https://www.epa.gov/); the ecoregions were: Mexican high plateau, eastern Sierra Madre
351   Oriental, west humid coastal plains and hills of the Gulf of Mexico, southern Sierra Madre del Sur,
352   east of the Mexican Plateau, east of the Trans Mexican Volcanic Belt, and south of the North
353   American deserts. These areas were chosen as likely accessible areas.
354   Values from the 19 current bioclimatic layers were extracted from individual occurrences
355   and Pearson's correlations threshold of 0.8 and 0.7 were performed with the occurrences sites to
356   minimize variable redundancy using NTBOX v0.1.4.5 R package (Osorio-Olvera et al., 2020).

357 The final uncorrelated variables according to the 0.8 Pearson's threshold were: annual mean
358 temperature (BIO1), isothermality (BIO3), temperature seasonality (BIO4), temperature annual
359 range (BIO7), annual precipitation (BIO12), precipitation of the driest month (BIO14),
360 precipitation seasonality (BIO15), and precipitation of the warmest quarter (BIO18). For the 0.7
361 threshold, BIO4 was the only variable discarded. To have a better balance between the number
362 of occurrences and the number of bioclimatic variables, the niche model was built with the 0.7
363 correlation threshold (Dormann et al., 2012) under the maximum entropy algorithm (Phillips et
364 al., 2017) in MAXENT v3.4.1 using the KUENM v1.1.1 R package (Cobos et al., 2019). Some
365 levels of model complexity were evaluated by varying the regularization multiplier (RM) from
366 0.5 to 10 every 0.5, and feature classes linear (L), quadratic (Q), product (P), and threshold (T) in
367 four fixed combinations: L, LQ, LQP, and LQPT, which resulted in 80 candidate niche models.
368 The hinge (H) feature was not considered to simplify the niche model for subsequent
369 transferability. The evaluation was made using 10,000 background points, five percent of
370 training data omission rate (OR), 20% for bootstrapping to calculate the partial Receiver
371 Operating Characteristic (pROC) with 10000 iterations. The best model was selected considering
372 the statistically significant models, and the lowest values of corrected Akaike information
373 criterion (AICc) and inspecting the OR. The average niche model with the best parameters was
374 built and projected to the same area using ten replicates of bootstrap and the logistic output
375 format.
376   To construct the paleodistributions, the 19 variables used for the current model were
377 downloaded, and the features of the best current niche model were projected to the same area
378 into past four scenarios based on the Community Climate System Model simulations. The
379 scenarios assessed were: mid-Holocene (MH; ~8.3 – 4,000 years ago (ya)) at 30 sec downloaded
380 from WORLDCLIM (http://www.worldclim.com), early-Holocene (EH; ~11.7 – 8,000 ya) at 2.5
381 min resolution (Fordham et al., 2017) downloaded from PALEOCLIM
382 (http://www.paleoclim.org/), Last Glacial Maximum (LGM; ~23 – 14,000 ya) at 30 sec
383 downloaded from CHELSA (Karger et al., 2018), and Last Interglacial (LIG; ~ 120 – 140,000
384 ya) at 30 sec (Otto-Bliesner, 2006) downloaded from WORLDCLIM. The resolution of EH was
385 downscaled to 30 sec. The extent and dimension of all scenarios were matched with those of the
386 current model to make further comparisons and avoid alterations in predictions (Randin et al.,
387 2009). The layer sources were chosen to have the original 30 sec resolution for most scenarios.
388   To evaluate the risk of extrapolating to non-analogous conditions (novel environments) in
389 each past scenario, we compare the calibration area (i.e., reference data) with the four past
390 scenarios (i.e., projection data) by quantifying the extrapolation due to covariate range (NT1) and
391 correlation change (NT2) with the ExDet method (Mesgaran et al., 2014) implemented in
392 NTBOX v0.1.4.5. Transferability was carried out using three methods of extrapolation: free
393 extrapolation, extrapolation and clamping, and no extrapolation. The niche overlap was
394 calculated using the Schoener's D metric in the geographic space (Warren et al., 2008), which D
395 values range from 0 (no overlap) to 1 (identical predictions). Finally, we calculated Pearson

396 correlations between model predictions. All procedures were performed in the R libraries raster
397 v3.3-13 (Hijmans, 2020) and ENMeval v0.3.0 (Muscarella et al., 2014).
398
399
400 **Results**
401
402 *Phylogenetic and haplotype relationships*
403
404 The phylogenetic cpDNA concatenated matrix including sequences from other *Magnolia* species
405 used as outgroup consisted of 106 individuals with a total length without gaps and missing data
406 of 2,803bp. The aligned matrix consisted of 147 polymorphic and 35 informative sites. The best-
407 fitting model of sequence evolution was GTR + I. The BI tree showed that *M. iltisiana, M.*
408 *pacifica, M. pedrazae, M. schiedeana* and *M. schiedeana* pop. Oaxaca formed a polytomy with a
409 low support (PP = 0.5). Samples from *M. pedrazae* and *M. schiedeana* were not monophyletic,
410 but samples from *M. schiedeana* pop. Oaxaca were grouped within well-supported subclade (PP
411 = 1) (Fig. 2A).
412   For the haplotype network, the concatenated cpDNA matrix had a total length of 2,858 bp
413 excluding gaps and missing data for 96 individuals. There were 47 polymorphic sites and 18
414 informative sites. A total of 49 haplotypes were identified (Table 1). Haplotype relationships
415 revealed only two shared haplotypes (H01 and H02) between *M. pedrazae* (north) and *M.*
416 *schiedeana* (central), and none with *M. schiedeana* pop. Oaxaca (south). Overall, few haplotypes
417 were shared among populations, but most of them diverged by one mutational change (max 5
418 mutation steps between H02 and H13 from *M. schiedeana*). The most frequent haplotypes (H02
419 and H03) were present in 7 out of 15 *M. schiedeana* populations, and present only (H02) in one
420 population from *M. pedrazae* in San Luis Potosí. Haplotype connections between *M. pedrazae*
421 and *M. schiedeana* occurred through haplotypes from Veracruz populations (MI (H36), FXC
422 (H22 and H23)), while the connection of the three *M. schiedeana* pop. Oaxaca haplotypes were
423 through a missing haplotype that tied a haplotype from *M. schiedeana* in Hidalgo (GO) and *M.*
424 *pedrazae* from San Luis Potosí and Querétaro (CS, JH) (Fig. 2B).

425

426 *Genetic diversity, phylogeographic structure and environmental differentiation*
427
428 Genetic diversity was high for *M. schiedeana* (Hd = 0.923; π = 0.001) and *M. pedrazae* (Hd =
429 0.95; π = 0.0009) and moderate for *M. schiedeana* pop. Oaxaca (Hd = 0.7; π = 0.0007). At the
430 level of populations, the most genetically diverse were MY and AC in Veracruz for *M.*
431 *schiedeana*, and CS in San Luis Potosí for *M. pedrazae* (Table 1). The AMOVA with no groups
432 defined a priori showed that the genetic variance explained among populations was 32.5% (F_{ST}=
433 0.33, P < 0.001). When populations were grouped in two lineages (*M. pedrazae* + *M.*
434 *schiedeana,* and *M. schiedeana* pop. Oaxaca), a much higher proportion of the genetic variance

435 and thus genetic differentiation was observed (57.6%, F_{CT} = 0.58, P < 0.001), whereas when
436 three lineages were considered (*M. pedrazae, M. schiedeana* and *M. schiedeana* pop. Oaxaca), a
437 slightly lower proportion of the genetic variance and genetic differentiation were observed
438 relative to the two lineages grouping (48.3%, F_{CT} = 0.48, P < 0.001) (Table 2). Pairwise F_{ST}
439 comparisons showed that the highest differentiation was between *M. schiedeana* and *M.*
440 *schiedeana* pop. Oaxaca (F_{ST} = 0.67, P = 0.001), and the lowest between *M. schiedeana* and *M.*
441 *pedrazae* (F_{ST} = 0.42, P = 0.001) (Supplemental Table S2). We found a weak and significant
442 pattern of IBD for the whole data set (r = 0.31, P = 0.022), but which significant effect
443 disappeared when *M. schiedeana* pop. Oaxaca was excluded from the analysis (r = 0.015, P =
444 0.46). Results from PERMUT revealed a significant phylogeographical structure (G_{ST} = 0.048
445 and N_{ST} = 0.364, P < 0.05).
446   BAPS revealed four likely clusters (K = 4, log marginal likelihood = -201.9484, PP =
447 0.72): cluster one was mostly formed by *M. pedrazae*, cluster 2 mostly with *M. schiedeana*,
448 cluster 3 with only one individual from GO, and cluster 4 with *M. schiedeana* pop. Oaxaca and
449 MI population; these observed clusters thus corresponded to the three TMCF regions (Fig 2C).
450 Similarly, BPEC showed three phylogeographic clusters with high membership posterior
451 probabilities for most haplotypes (PP = 0.80 to 0.99). The three main clusters also corresponded
452 to *M. pedrazae, M. schiedeana* and *M. schiedeana* pop. Oaxaca (Fig. 2D). However, uncertainty
453 of cluster location was evident for the *M. schiedeana* pop. Oaxaca, as some *M. schiedeana*
454 haplotypes (H10, H17, H22, H23, H36, H40) from Veracruz (except H10 from Puebla) were
455 assigned to *M. schiedeana* pop. Oaxaca (Supplemental Fig S1). Ancestral locations were in
456 central Veracruz (Supplemental Fig S1). The environmental variation of the two PCs revealed
457 statistically significant differences among the three lineages (Pillai´s trace = 0.78, $F_{2,93}$ = 30.21,
458 P < 0.001). Tukey-HSD revealed statistically significant pairwise differences between the three
459 lineages along the PC 1 (38.3% P < 0.001); variable contribution was: temperature annual range
460 (BIO7) = 27.3%, precipitation seasonality (BIO15) = 24.2%, temperature seasonality (BIO4) =
461 21.3% and precipitation of the driest month (BIO14) = 20.3%). For the PC 2 (28.4%) statistically
462 significant differences were observed between *M. schiedeana* and *M. pedrazae* (P < 0.001) and
463 between *M. schiedeana* and *M. schiedeana* pop. Oaxaca (P < 0.001); variable contribution was:
464 annual precipitation (BIO12) = 34.6%, precipitation of the warmest quarter (BIO18) = 34.2%,
465 and precipitation of the driest month (BIO14) = 13.2% (Fig. 2E-F).

466

467 *Historical demographic changes*

468

469 Tajima's D and Fu´s F showed statistically significant negative values, and positive significant
470 *R2* values for *M. schiedeana*, indicative of population expansion, while for *M. pedrazae* and *M.*
471 *schiedeana* pop. Oaxaca, neutrality tests were non-significant (Table 3). Mismatch distributions
472 for the observed and expected values for *M. pedrazae* and *M. schiedeana*, fit with the expectation
473 of recent demographic expansions (Fig. 3A and 3B). These mismatch distributions were not
474 rejected by the SSD and Hri tests (Table 3). Bayesian skyline plots of N_e through time showed an

475   increase in effective population size over time for *M. pedrazae* at ~ 200,000 years ago (Fig. 3C),
476   and for *M. schiedeana* between ~ 300,000 to 250,000 years ago (Fig. 3D), both predating the
477   LGM.
478   The ABC simulations provided the best support for scenario 2 and scenario 5 (PP: 0.35,
479   95% CI: 0.342–0.366 and PP: 0.36, 95% CI: 0.347–0.373, respectively) that performed better than
480   the other three scenarios. Confidence estimates for scenario choice indicated that Type I errors for
481   the best-supported scenarios were high (scenario 2: 0.62 and scenario 5: 0.64) but Type II errors
482   were higher for scenario 5 (0.73) relative to the scenario 2 (0.51). As statistically there is no way to
483   discriminate which of the two is the best scenario when both are equally likely (Bertorelle et al.,
484   2010), we considered scenarios 2 and 5 as the most likely, although biologically they are
485   contrasting (Fig. 4). Assuming a 10-year generation time, under scenario 2 and 5, the posterior
486   mean parameter estimates indicated that the divergence (t_2) of *M. schiedeana* pop. Oaxaca from *M.*
487   *schiedeana* occurred 82,300 (CI: 37.7–99.2) and 84,800 (CI: 41.7-99.4) years ago, respectively,
488   which fits the LIG. Under scenario 2, the mean estimated divergence time of *M. schiedeana* and *M.*
489   *pedrazae* was 35,000 (CI: 3.5–81.3) years ago before the LGM, while for scenario 5, the admixture
490   among the tree lineages was estimated around 22,900 (CI: 1.7–72.7) years ago, during the LGM.
491   However, confidence intervals were large for both scenarios, going from the LIG until very recent
492   times (Supplemental Table S3 and Fig S2).
493
494   *Present and past species distributions*
495
496   The evaluation showed that the best niche model has a significant pROC (*P* < 0.001), 0.22 OR,
497   and 1617.9 AICc with the LQP features and 1.0 RM. This niche model was constructed with the
498   following variables and permutation importance: BIO14 (39%), BIO1 (34%), BIO3 (10.7%),
499   BIO7 (6.2%), BIO18 (4.8%), BIO12 (2.7%), and BIO15 (2.7%).
500   The present niche model geographically projected showed the highest suitability values
501   mainly at the center of Veracruz and for scattered areas towards the northern periphery, while
502   Oaxaca showed moderate suitability values (Fig. 5A-B). The extrapolation detection analyses
503   showed that the percentage of non-analogous conditions for each past scenario were: NT1
504   (34.5%) and NT2 (3.24%) for MH, NT1 (4%) and NT2 (0.25%) for EH, NT1 (8.4%) and NT2
505   (0.13%) for LGM, and NT1 (24.9%) and NT2 (0.19%) for LIG. The NT1 and NT2 extreme
506   values were low (-2.4 and -7.9) confirming low extrapolation risk (Supplemental Fig S3). On the
507   other hand, the three methods of extrapolation for the four past scenarios showed similar
508   predictions with only slight variations, therefore, only the projections with no extrapolation are
509   shown.
510   Paleodistributions to the MH revealed that high suitability values were present in scarce
511   areas at central east of the TMCF (Puebla and Veracruz) (Fig. 5C), whereas for the EH much
512   higher suitability values were found across most of the species ranges from north (San Luis
513   Potosí), central (Veracruz) and south (Oaxaca) (Fig. 5D). During the LGM high suitability
514   habitat was present in two disconnected areas, one in central Veracruz and the other in south of

515   Oaxaca (Fig. 5E). During the LIG, a thin strip with high suitability was restricted mostly at the
516   central east (Veracruz and Puebla) (Fig. 5F). The Schoener's D and Pearson correlation between
517   the present and past species projections were MH: D = 0.2 and r = 0.24, EH: D = 0.47 and r =
518   0.56, LGM: D = 0.48 and r = 0.53, and LIG: D = 0.49 and r = 0.69, which highlights the
519   differences between the present and past niche suitability species distributions.
520
521
522   **Discussion**
523
524   In this study we employed analysis of phylogeography, historical demography and
525   paleodistributions to understand how climatic oscillations of the Pleistocene have shaped
526   geographical patterns of genetic diversity in endemic *Magnolia* trees of the largest remaining
527   TMCF strip in Mexico. Based on four cpDNA sequences, we found evidence of three genetic
528   lineages and signatures of demographic expansions, while past species distributions showed
529   range expansions and contractions during the interglacial-glacial cycles of the Pleistocene, which
530   suggest the strong role of climatic and/or environmental factors influencing the complex
531   evolutionary dynamics of these *Magnolia* lineages.
532
533   *Genetic differentiation among TMCF regions*
534
535   The MJ network, BAPS, and BPEC analyses jointly revealed three genetic clusters that showed a
536   significant phylogeographical structure. The MJ network revealed 10 haplotypes exclusive to the
537   north (*M. pedrazae*), 34 haplotypes to the central (*M. schiedeana*), and three to the south (*M.*
538   *schiedeana* pop. Oaxaca) of the TMCF. Only two haplotypes were shared between the north and
539   central lineages, one of which was widespread in the central region but not in the north. None of
540   the haplotypes were shared between *M. schiedeana* pop. Oaxaca. Similarly, AMOVAs showed
541   that the amount of genetic variance explained among these three lineages was moderate (48%),
542   but it was considerable higher (58%) when only two lineages (*M. pedrazae + M. schiedeana* and
543   *M. schiedeana* pop. Oaxaca) were considered. In contrast to these results, the Bayesian
544   phylogenetic tree did not resolve the monophyly of the three lineages as all samples formed a
545   polytomy with other closely related *Magnolia* species (*M. iltisiana* and *M. pacifica*). The lack of
546   resolution of the phylogenetic relationships based on the cpDNA may be due to its slow-evolving
547   mutation rate (Richardson et al., 2013) and incomplete lineage sorting, which has been found in
548   other magnolias (Kikuchi & Osone, 2021). On the other hand, the chloroplast DNA in magnolias
549   is maternally inherited (Tobe et al., 1993) and thus reflect patterns of seed-mediated gene flow.
550   Bird dispersal as likely occurs for *M. schiedeana* (Watanabe et al., 2002) may provide gene flow
551   at large spatial scales thus connecting populations over large distances (Newton et al., 2008;
552   Setsuko & Tomaru, 2009).
553   The geographical circumscription of *M. schiedeana* has changed over time as the result of
554   recent species designations based on morphological characters (Jiménez-Ramírez et al., 2007;

555   Cruz-Durán et al., 2008; Vázquez-García et al., 2012; Vázquez-García et al., 2013), while
556   molecular taxonomic studies are lacking. A population genetic study by Rico & Gutiérrez-
557   Becerril (2019) pointed that the species designation of *M. pedrazae* was not evident based on
558   observed patterns of genetic differentiation estimated with nuclear microsatellites that showed
559   strong to moderate differentiation across populations irrespective of their species identity.
560   Although few populations of *M. schiedeana* were included in the study. For populations in
561   Oaxaca, specifically in Santiago Comaltepec, the taxonomic designation remains unclear. Our
562   results clearly support the genetic divergence of *M. schiedeana* pop. Oaxaca, which likely has
563   remained isolated for a longer time according to the ABC analysis and the largest differentiation
564   of this population shown by the pairwise F_{ST} estimates. Due to our limited sampling for Oaxaca,
565   we cannot confirm if this population represents a distinct taxonomic unit. A formal taxonomic
566   delimitation study between *M. schiedeana* and recent designated species is outside the scope of
567   this work. Species designation and delimitation remain controversial topics in biology (De
568   Queiroz, 2007) and the taxonomy of Neotropical magnolias is a good example of the complexity
569   to circumscribe species (Vázquez-García, 1994; Aldaba-Núñez et al., 2021). However, as
570   recently suggested by Huang (2020), to clarify whether population subdivision or speciation is
571   warranted from an evolutionary perspective, we need a better understanding of the sources that
572   generate and maintain structured intraspecific variation that may lead to interspecific divergence.
573   In this study we contribute towards understanding the historical processes that have shaped
574   pattens of genetic diversity in these *Magnolia* populations. Additional morphological, molecular
575   (nuclear markers) and ecological data and broader population sampling is needed to further
576   clarify species delimitation of the *Magnolia* section.
577
578   *Effects of the Pleistocene in the phylogeographical structure and demographic changes*
579
580   Divergence among Neotropical magnolias is thought to occur mainly by vicariance given by the
581   archipelago-type distribution of the TMCF (Vázquez-García, 1994; Jiménez-Ramírez et al.,
582   2007; Cruz-Durán et al., 2008). Phylogeographical studies of tree species of the TMCF in
583   Mexico have shown patterns of allopatric divergence caused by major biogeographical barriers,
584   such as the Trans-Mexican Volcanic Belt (TMVB) (*Liquidambar styraciflua*, Ruiz-Sánchez &
585   Ornelas, 2014) and for the Isthmus of Tehuantepec (*Palicourea padifolia*, Gutiérrez-Rodríguez
586   et al., 2011) during the Pliocene to mid-Pleistocene. Specifically, the TMVB is a volcanic chain
587   that horizontally splits Mexico into north and south, and which has profound impacts on the
588   historical differentiation across multiple taxa, including flora and fauna (Mastretta-Yañes et al.
589   2015). The diversification of the *Magnolia* section has been estimated around 32.4 Mya at the
590   early Oligocene, while the divergence of *M. schiedeana* can be placed at ~10 Mya during the late
591   Miocene (Dong et al., 2021). This epoch was marked by the second pulse of volcanism from
592   west to east of the TMVB (~ 11 to 7 Mya, Ferrari et al., 2012), and by warm and humid
593   conditions (Frigola et al., 2018). However, the estimated divergence based on the ABC analyses
594   was far more recent; scenario 2 suggests that *M. schiedeana* pop. Oaxaca is the oldest lineage

595   that diverged from a common ancestor around 80,000 years ago, while scenario suggests that *M.*
596   *schiedeana* and *M. schiedeana* pop. Oaxaca diverged from a common ancestor around 85,000
597   years ago, both estimations of divergence events occurred during the warm and wet conditions of
598   the LIG. The BPEC analyses suggested that ancestral haplotypes were in central Veracruz, and
599   this coincides with the past niche projections where the largest extent of optimal habitat occurred
600   in this region during the LIG. Our small sample size for *M. pedrazae* and *M. schiedeana* pop.
601   Oaxaca, and the large confidence intervals obtained from demographic analyses, suggest that our
602   divergence and demographic expansion dates should be interpreted cautiously. Moreover, the
603   ABC simulations showed as equally likely two contrasting demographic scenarios, one that
604   suggested the divergence of the three lineages, and the other their admixture, which we could not
605   discriminate given their high type I and II error rates.
606   Neutrality tests showed demographic expansions for *M. schiedeana*, while the mismatch
607   distributions and the star-shape topology of the haplotype network suggested that *M. pedrazae*
608   also underwent a demographic expansion. These observations agreed with the Bayesian skyline
609   plots that showed demographic expansions for *M. schiedeana* (~ 250,000 ya) and *M. pedrazae* (~
610   200,000 ya), both predating the LIG. Demographic growth was also suggested by the ABC
611   simulations, which showed an increase of population sizes for both scenarios after the divergence
612   from a common ancestor around the LIG (Supplemental Table S3). Our paleodistribution models
613   during the last ~120,000 years ago highlighted complex population dynamics characterized by
614   range shifts, contractions-expansions. Specifically, during the warmer conditions of the LIG,
615   suitable habitat was mainly restricted to central Veracruz and Puebla, Then, during the LGM,
616   suitable habitat remained in Veracruz and Puebla, but also was present in south of Oaxaca,
617   although both areas were disconnected. Later during the early Holocene, suitable habitat
618   considerably expanded northwards, from Oaxaca to Veracruz and San Luis Potosí. However, in
619   the mid-Holocene suitable habitat was drastically reduced to small areas in Puebla and Veracruz,
620   and then expanded in the present. Although our past scenarios were well supported and showed
621   low extrapolation risk, caution must be warranted considering the low number of occurrences
622   used to build the niche model and that these hypotheses are based on a single GCM, specifically
623   in the LGM in which different GCM could give contrasting results (Guevara et al. 2018).
624   Increasing the number of occurrence records through field explorations and taxonomic studies in
625   these taxa would further improve the accuracy of species distribution models.
626   The glacial refugia proposed by Toledo (1982), suggests that Sierra de Juárez in Oaxaca
627   and Córdoba in Veracruz were secondary refugia for tropical forest species during the LGM due
628   to their high humid conditions. For instance, the Sierra de Juárez in Santiago Comaltepec is
629   recognized as one of the TMCF regions where atmospheric humidity is the highest (Gual-Díaz &
630   González-Medrano 2014). The secondary refugia suggested by Toledo coincides with the
631   locations of high suitable habitat predicted for the LGM, one towards the south of Oaxaca and
632   the other in central Veracruz, although suitable habitat during the LGM increased relatively to
633   the LIG, which the refugia model do not predict. As there is no conclusive evidence
634   unambiguously supporting either of the two precipitation models, further investigations are

635   needed by incorporating more samples (Oaxaca) and highly variable nuclear markers for testing
636   these and other alternative hypotheses (vulcanism in the TMVB), which could elucidate the
637   complex evolutionary history of these lineages.
638   According to our genetic data, *Magnolia schiedeana* pop. Oaxaca likely remained
639   isolated from the other two lineages before and during the LGM, as suggested by the lack of
640   shared haplotypes among them and the evidence of its oldest divergence relative to the other two
641   lineages. During the early Holocene (~ 11. 7 ya) the increase in temperature and humidity could
642   have facilitated the range expansion from the south-central towards the northern periphery.
643   Colonization of the northern periphery may have occurred by long-distance dispersal as
644   suggested by the lack of IBD between *M. pedrazae* and *M. schiedeana*, and the retention of
645   ancestral polymorphism in the cpDNA. The star-like network topology, the high haplotype
646   diversity, but the low nucleotide diversity suggests the most recent recolonization of the northern
647   periphery of the TMCF. The range contraction-expansion from the mid-Holocene (~ 8.3 ya) to
648   the present suggested by the climatic models, may explain the weaker genetic divergence
649   between *M. pedrazae* and *M. schiedeana* as there is no major geographical barriers that could
650   explain their genetic divergence. Moreover, the BPEC analysis suggested that genetic divergence
651   can also be shaped by environmental factors. Specifically, the environmental PCAs revealed
652   significant differences among the three lineages, which mainly can be attributed to annual
653   temperature range and precipitation seasonality. The TMCF of Mexico are composed of highly
654   heterogenous forest that can vary markedly in environmental conditions (Gual-Díaz & González-
655   Medrano 014). Local environmental differences have been suggested to generate the large
656   intraspecific morphological variations observed across populations of *M. schiedeana* (Vite et al.,
657   2016; Rodríguez-Ramírez et al., 2020). This environmental heterogeneity may have led to
658   differential habitats preferences and thus to divergence by ecological factors, a potential
659   hypothesis that could be tested in the future.
660
661
662   *Conservation implications*
663
664   The TMCF is one of the most threatened ecosystems due to the strong anthropogenic pressures
665   for land conversion and the predicted changes in temperature and precipitation regimes due to
666   climate change (Toledo-Aceves et al., 2011; Ponce-Reyes et al., 2012). In Mexico, around 90%
667   of *Magnolia* species are vulnerable to extinction by habitat loss and fragmentation, and these
668   include *M. pedrazae* and *M. schiedeana* (Rivers et al., 2016). Genetic diversity estimates showed
669   that San Luis Potosí is the most diverse region for *M. pedrazae*, and central Veracruz for *M.
670   schiedeana*. However, only few of these studied localities (e.g., CS and MA) are large
671   populations (> 300 individuals), while most of them are small (< 100 individuals, e.g., JH, FO,
672   TU, MM, CP, MA). In fact, we found localities where the species might be locally extinct, such
673   as TLA in Puebla and MI in Veracruz, as we found a single remaining individual. The TMCF of
674   San Luis Potosí and Veracruz are under strong anthropogenic pressures from ongoing land-

675 conversion to agriculture and livestock farming (CONABIO, 2010). Moreover, several
676 populations do not occur under Protected Natural Areas, such as the most genetically diverse
677 populations in Veracruz. Protecting and restoring TMCF habitat is crucial for the conservation of
678 *Magnolia* species (Rivers et al., 2016). This can be accomplished through implementing
679 community-based management strategies, such as the promotion of sustainable and
680 environmentally friendly tourism that can benefit the local communities. There are already
681 successful examples of community-based programs in large remnant TMCF fragments of San
682 Luis Potosí (La Trinidad) and Oaxaca (La Esperanza) that have large *Magnolia* populations (e.g.,
683 FO, CS, SI, SC), and where local communities host ecotourist destinations and agreed the
684 protection of their well-conserved forests forbidding commercial wood extraction.
685   On the other hand, our niche species distributions suggest that magnolias are sensitive to
686 climatic events since historical times, which lead to range shifts, expansions, and contractions.
687 Future climatic scenarios suggest a decrease of *M. schiedeana* suitable habitat by 2080
688 (Vázquez-Morales et al., 2014). Conserving genetic diversity of ancestral populations would be
689 important for the species conservation as ancestral populations are sources of evolutionary
690 adaptive potential (Frankham, 2005). According to our results, we suggest that special attention
691 should be paid to populations in central Veracruz, as these are likely the most ancestral
692 populations and where *M. schiedeana* is abundant in some localities; the same applies for the
693 northern periphery in San Luis Potosí. Monitoring genetic diversity and evaluating the role of
694 geographical and environmental factors on genetic diversity and gene flow would also be key for
695 the *in-situ* species management in the long-term.
696
697 **Acknowledgments**
698
699 We thank Bruno A. Gutiérrez Becerril, Sergio Nicasio Arzeta, and Benjamín Castillo Ponce for
700 their assistance in collecting leaf material. We also thank the useful comments from three
701 anonymous reviewers that improved the quality of our work during the revision stage.
702
703 **References**
704

705 Aiello-Lammens ME, Boria RA, Radosavljevic A, Vilela B, Anderson RP. 2015. spThin: an R
706   package for spatial thinning of species occurrence records for use in ecological niche
707   models. *Ecography* **38**:541–545.
708 Alcántara O, Luna I, Velázquez A. 2002. Altitudinal distribution patterns of Mexican cloud
709   forests based upon preferential characteristic genera. *Plant Ecology* **161**: 167-174.
710 Aldaba-Núñez FB, Veltjen E, Martínez-Salas EM, Samain MS. 2021. *Plants* **10**: 573
711 Azuma H, Chalermglin P, Nooteboom HP. 2011. Molecular phylogeny of Magnoliaceae based
712   on plastid DNA sequences with special emphasis on some species from continental
713   Southeast Asia. *Botany* **39**:148-165.
714 Bertorelle G, Benazzo A, Mona S. 2010. ABC as a flexible framework to estimate demography

715   over space and time: some cons, many pros. *Molecular Ecology* **19**: 2609-2625.

716 Cobos ME, Peterson AT, Barve N, Osorio-Olvera L. 2019. kuenm: an R package for detailed

717   development of ecological niche models using Maxent. *PeerJ* **7**:e6281.

718 CONABIO. 2010. El Bosque Mesófilo de Montaña en México: Amenazas y Oportunidades para

719   su Conservación y Manejo Sostenible. Comisión Nacional para el Conocimiento y Uso de la

720   Biodiversidad, México. 197 p.

721 Corander J, Sirén J, Arjas E. 2008. Bayesian spatial modeling of genetic population structure.

722   Computational Statistics. **23**:111–129.

723 Cornuet JM, Santos F, Beaumont MA, Robert CP, Marin JM, Balding DJ, Guillemaud T, Estoup

724   A. 2008. Inferring population history with DIY ABC: a user-friendly approach to

725   approximate Bayesian computation. *Bioinformatics*.**24**:2713–9.

726 Cornuet JM, Pudlo P, Veyssier J, Dehne-Garcia A, Gautier M, Leblois R, Marin JM, Estoup A.

727   2014. DIYABC v2.0: a software to make approximate Bayesian computation inferences

728   about population history using single nucleotide polymorphisms, DNA sequence and

729   microsatellite data. *Bioinformatics* **30**: 1187–1189.

730 Cruz-Cárdenas G, Villaseñor JL, López-Mata L, Ortiz, E. 2012. Potential distribution of humid

731   mountain forest in Mexico. *Botanical Sciences* **90**: 331–340.

732 Cruz-Durán R, Vega-Flores K, Jiménez-Ramírez J. 2008. *Magnolia vazquezii* Magnoliaceae, una

733   especie nueva del estado de Guerrero, Mexico. *Novon: A Journal for Botanical*

734   *Nomenclature* **18**:21–24.

735 D´Amen, M., Zimmermann, N. E., Pearman, P. B. 2013. Conservation of phylogeographic

736   lineages under climate change. *Global Ecology and Biogeography*, **22**:93-104.

737 Dalmaris E, Ramalho CE, Poot P, Veneklaas EJ, Byrne M. 2015. A climate change context for

738   the decline of a foundation tree species in south-western Australia: insights from

739   phylogeography and species distribution modeling. *Annals of Botany* **116**: 941-952.

740 Darriba D, Taboada GL, Doallo R, Posada D. 2012. jModelTest 2: more models, new heuristics

741   and parallel computing. *Nature Methods* **9:**772.

742 De Queiroz K. 2007. Species concepts and species delimitation. *Systematic Biology* **56**: 879-886.

743 Di Febbraro M. Carotenuto F, Castiglione S, Russo D, Loy A, Maiorano L, Raia P. 2017. Does

744   the jack of all trades fare best? Survival and niche width in Late Pleistocene

745   megafauna. *Journal of Biogeography* **44**:2828-2838.

746 Dieringer G, Espinosa SJE. 1994. Reproductive ecology of *Magnolia schiedeana* Magnoliaceae

747   a threatened cloud forest tree species in Veracruz, Mexico. *Bulletin of the Torrey*

748   *Botanical Club* **121**:154–159.

749 Dong S, Wang Y, Xia N, Liu Y, Liu M, Lian L, Li N, Li L, Lang X, Gong Y, Chen L, Wu E,

750   Zhang S. 2021. Plastid and nuclear phyligenomic incrongruences and biogeographic

751   implications of Magnolia s.l. (Magnoliaceae). *Journal of Systematics and Evolution*. doi:

752   10.111/jse.12727.

753 Dormann CF, Elith J, Bacher S, Buchmann C, Carl G, Carré G, García-Marquez JR, Gruber B,

754   Lafourcade B, Leitao PJ, Munkemuller T, McClean C, Osborne PE, Reineking B,

755   Schroder B, Skidmore AK, Zurell D, Lautenbach S. 2012. Collinearity: a review of
756   methods to deal with it and a simulation study evaluating their performance. *Ecography*
757   **36**: 27-46.
758   Doyle JJ, Doyle JL. 1987. A rapid DNA isolation procedure for small quantities of fresh leaf
759   tissue. *Phytochemical Bulletin* **19**:11–15.
760   Drummond AJ, Bouckaert RR. 2015. Bayesian evolutionary analysis with BEAST2 Cambridge
761   University Press, Cambridge, UK.
762   Edgar RC. 2004. MUSCLE: multiple sequence alignment with high accuracy and high
763   throughput. *Nucleic Acids Research* **32**:1792–1797.
764   Excoffier L, Fol M, Petit RJ. 2009. Genetic consequences of range expansions. *Annual Review of*
765   *Ecology, Evolution, and Systematics* **40**:481–501.
766   Excoffier L, Lischer H. 2010. Arlequin suite ver 3.5: a new series of programs to perform
767   population genetics analyses under Linux and Windows. *Molecular Ecology Resources*
768   **10:**564–567.
769   Ferrari L, Orozco-Esquivel MT, Manea V, Manea M. 2012. The dynamic history of the Trans-
770   Mexican Volcanic Belt and the Mexico subduction zone. *Tectonophysics.* **522–523***:* 122-
771   149
772   Fordham DA, Saltré F, Haythorne S, Wigley TML, Otto-Bliesner BL, Chan KC, Brook BW.
773   2017. PaleoView: a tool for generating continuous climate projections spanning the last
774   21 000 years at regional and global scales. *Ecography* **40**:1348–1358.
775   Frankham R. 2005. Genetics and extinction. *Biological Conservation, 126*: 131-140.
776   Frigola A, Prange M, Schulz M. 2018. Boundary conditions for the middle Miocene climate
777   transition MMCT v1.0. *Geoscientific Model Development* **114**:1607-1626.
778   Fu YX, 1997. Statistical tests of neutrality of mutations against population growth, hitchhiking
779   and background selections. *Genetics* **174**: 918–925.
780   Galante PJ, Alade B, Muscarella R, Jansa SA, Goodman SM, Anderson RP. 2018. The challenge
781   of modeling niches and distributions for data-poor species: a comprehensive approach to
782   model complexity. *Ecography* **41**:726–736
783   González-Espinosa M, Meave JA, Lorea-Hernández FG, Ibarra-Manriquez G, Newton AC.
784   2011. The red list of Mexican Cloud Forest trees. Fauna and Flora International,
785   Cambridge
786   Graham A. 1999. Studies in Neotropical paleobotany. XIII. An Oligo-Miocene palynoflora from
787   Simojovel Chiapas, Mexico. *American Journal of Botany* **86**:17–31.
788   Gual-Díaz M, González-Medrano F. 2014. Los bosques mesófilos de montaña de México. Gual-
789   Díaz, M. & A. Rendón-Correa (eds) In: Bosques Mesófilos de Montaña de México:
790   diversidad, ecología y manejo. Comisión Nacional para el Conocimiento y Uso de la
791   Biodiversidad. México, DF, México, 189-196.
792   Guevara L, Morrone JJ, León-Paniagua L. 2018. Spatial variability in species' potential
793   distributions during the Last Glacial Maximum under different Global Circulation

794   Models: relevance in evolutionary biology. *Journal of Zoological Systematics and*
795   *Evolutionary Research* **57**:113–126.

796 Guevara L. 2020. Altitudinal, latitudinal and longitudinal responses of cloud forest species to
797   Quaternary glaciations in the northern Neotropics. *Biological Journal of the Linnean*
798   *Society.* **130**: 615–625.

799 Gutiérrez-Rodríguez C, Ornelas JF, Rodríguez-Gómez F. 2011. Chloroplast DNA
800   phylogeography of a distylous shrub *Palicourea padifolia*, Rubiaceae reveals past
801   fragmentation and demographic expansion in Mexican cloud forests. *Molecular*
802   *Phylogenetics and Evolution* **61**: 603-615.

803 Harpending H, Batzer M, Gurven M, Jorde L, Rogers A, Sherry S. 1998. Genetic traces of
804   ancient demography. *Proceedings of the National Academy of Sciences of the United*
805   *States of America.* **95**:1961–1967.

806 Hebda RJ, Irving E. 2004. On the origin and distribution of magnolias: tectonics, DNA and
807   climate change. In: Channell JET, Kent DV, Lowrie W, Meert JG (eds) Timescales of the
808   paleomagnetic field. Greophysical monograph series 145. American Geophysical Union,
809   Washington DC, pp 43–57.

810 Hijmans RJ. 2020. raster: geographic data analysis and modeling. R package version 3.3-13.
811   https://CRAN.R-project.org/package=raster

812 Huang JP. 2020. Is population subdivision different from speciation? From phylogeography to
813   species delimitation. *Ecology and Evolution* **10:**6890-6896.

814 Huelsenbeck JP, Ronquist F. 2001. MrBayes: Bayesian inference of phylogenetic trees.
815   *Bioinformatics* **17**:754–755

816 Jiménez-Ramírez J, Vega-Flores K, Cruz-Durán R, Vázquez-García JA. 2007. Una nueva
817   especie del bosque mesófilo de montaña del estado de Guerrero, México. *Botanical*
818   *Sciences* **80**:73–76

819 Karger DN, Conrad O, Böhner J, Kawohl T, Kreft H, Soria-Auza RW, Zimmermann NE, Linder
820   HP, Kessler M. 2017. Climatologies at high resolution for the earth's land surface areas.
821   *Scientific Data* **4**:170122.

822 Karger DN, Conrad O, Böhner J, Kawohl T, Kreft H, Soria-Auza RW, Zimmermann NE, Linder
823   HP, Kessler M. 2018. Data from: Climatologies at high resolution for the earth's land
824   surface areas. Dryad Digital Repository. http://dx.doi.org/doi:10.5061/dryad.kd1d4

825 Kikuchi S, Osone Y. 2021. Subspecies divergence and pronounced phylogenetic incongruence in
826   the East-Asia-endemic shrub *Magnolia sieboldii*. *Annals of Botany* 127: 75-90

827 Kumar S, Stecher G, Li M, Knyaz C, Tamura K. 2018. MEGA X: molecular evolutionary
828   genetics analysis across computing platforms. Molecular Biology and Evolution.
829   **35**:1547-9.

830 Leigh JW, Bryant D. 2015. Popart: full-feature software for haplotype network construction.
831   *Methods in Ecology and Evolution* **6**:1110–1116.

832 Manolopoulou I, Emerson BC. 2012. Phylogeographic ancestral inference using the coalescent
833   model on haplotype trees. *Journal of Computational Biology*. **19**:745-55.

834   Manolopoulou I, Hille A, Emerson BC. 2020. BPEC: An R package for Bayesian
835   phylogeographic and ecological clustering. *Journal of Statistical Software* **92**: 1-32
836   Manolopoulou I, Legarreta L, Emerson BC, Brooks S, Tavaré S. 2011. A Bayesian approach to
837   phylogeographic clustering. *Interface focus* **1**: 909-921.
838   Mastretta-Yanes A, Moreno-Letelier A, Piñero D, Jorgensen TH, Emerson BC. 2015.
839   Biodiversity in the Mexican highlands and the interaction of geology, geography and
840   climate within the Trans-Mexican Volcanic Belt. *Journal of Biogeography* **42**:1586-
841   1600.
842   Mesgaran MB, Cousens RD, Webber BL. 2014. Here be dragons: a tool for quantifying novelty
843   due to covariate range and correlation change when projecting species distribution
844   models. Diversity and Distributions **20**: 1147-1159.
845   Muscarella R, Galante PJ, Soley-Guardia M, Boria RA, Kass JM, Uriarte M, Anderson RP.
846   2014. ENMeval: an R package for conducting spatially independent evaluations and
847   estimating optimal model complexity for Maxent ecological niche models. *Methods in
848   Ecology and Evolution* **5**:1198–1205.
849   Nakazato T, Warren DL, Moyle LC. 2010. Ecological and geographic modes of species
850   divergence in wild tomatoes. *American Journal of Botany* **97**:680-693.
851   Newton AC, Robertson A, Williams-Linera G, Rámirez-Marcial N, González-Espinosa M,
852   Allnutt TR, Ennos R 2007 Genetic variation in two rare endemic mexican trees,
853   *Magnolia sharpii* and *Magnolia schiedeana*. *Silvae Genetica* **57**:348–356
854   Oksanen J, Blanchet FG, Kindt R, Legendre P, Minchin PR, O'Hara RB, Simpson GL, Solymos
855   P, Stevens MH, Wagner H. 2015. Vegan: Community ecology package. Ordination
856   methods, diversity analysis and other functions for community and vegetation ecologist. R
857   package version. **2015**:2-3
858   Ornelas JF, Ortiz-Rodriguez AE, Ruiz-Sanchez E, Sosa V, Pérez-Farrera MA. 2019. Ups and
859   downs: genetic differentiation among populations of the *Podocarpus* Podocarpaceae species
860   in Mesoamerica. *Molecular Phylogenetics and Evolution* **138**:17-30.
861   Ornelas JF, Sosa V, Soltis DE, Daza JM, González C, Soltis PS, Gutiérrez-Rodríguez C,
862   Espinoza de los Monteros AE, Castoe TA, Bell C, Ruiz-Sanchez E. 2013. Comparative
863   phylogeographic analyses illustrate the complex evolutionary history of threatened cloud
864   forests of northern Mesoamerica. *PloS One* **8**: e56283.
865   Osorio-Olvera L, Lira-Noriega A, Soberón J, Peterson AT, Falconi M, Contreras-Díaz RG,
866   Martínez-Meyer E, Barve V, Barve N. 2020. NTBOX: An r package with graphical user
867   interface for modeling and evaluating multidimensional ecological niches. *Methods in
868   Ecology and Evolution* **11**:1199-206
869   Otto-Bliesner BL. 2006. Simulating arctic climate warmth and icefield retreat in the last
870   interglaciation. *Science* **311**:1751–1753.
871   Paradis E. 2010. pegas: an R package for population genetics with an integrated–modular
872   approach. *Bioinformatics* **26**:419-420.

873   Phillips SJ, Anderson RP, Dudík M, Schapire RE, Blair ME. 2017. Opening the black box: an
874   open-source release of Maxent. *Ecography* **40**:887–893.
875   Pineda E, Moreno C, Escobar F, Halffter G. 2005. Frog, bat, and dung beetle diversity in the
876   cloud forest and coffee agroecosystems of Veracruz, Mexico. *Conservation Biology*
877   **19**:400-410.
878   Ponce-Reyes R, Reynoso-Rosales VH, Watson JE, VanDerWal J, Fuller RA, Pressey RL,
879   Possingham HP. 2012. Vulnerability of cloud forest reserves in Mexico to climate
880   change. *Nature Climate Change* **2**:448-452.
881   Pons O, Petit RJ. 1996. Measuring and testing genetic differentiation with ordered versus
882   unordered alleles. *Genetics* **144**:1237–1245.
883   Prance G. 1982. A Review of the phytogeographic evidences for Pleistocene climate changes in
884   the neotropics. *Annals of the Missouri Botanical Garden* **69**:594-624.
885   R Core Team. (2020). R: A Language and Environment for Statistical Computing. Vienna,
886   Austria. Retrieved from https://www.R-project.org/
887   Rahbek C, Borregaard MK, Antonelli A, Colwell RK, Holt BG, Nogues-Bravo D, Rasmussen
888   CM, Richardson K, Rosing MT, Whittaker RJ Fjeldså J. 2019. Building mountain
889   biodiversity: Geological and evolutionary processes. *Science* **365**:1114-1119.
890   Rambaut A, Drummond AJ, Xie D, Baele G, Suchard MA. 2018. Posterior summarisation in
891   Bayesian phylogenetics using Tracer 1.7. *Systematic Biology*. **67**:901.
892   Ramírez-Barahona S, Eguiarte LE. 2013. The role of glacial cycles in promoting genetic
893   diversity in the Neotropics: the case of cloud forests during the Last Glacial
894   Maximum. *Ecology and Evolution* **3:**725-738.
895   Ramírez-Barahona S, Sauquet H, Magallón S. 2020. The delayed and geographically
896   heterogenous diversification of flowering plant families. *Nature Ecology and Evolution* **4**:
897   1232-1238
898   Ramos-Onsins SE, Rozas J. 2002. Statistical properties of new neutrality tests against population
899   growth. *Molecular Biology and Evolution* **19**: 2092-2100.
900   Randin CF, Engler R, Normand S, Zappa M, Zimmermann NE, Pearman PB, Vittoz P, Thuiller
901   W, Guisan A. 2009. Climate change and plant distribution: local models predict high-
902   elevation persistence. Golbal Chance Biology **15**:1557-1569.
903   Richardson AO, Rice DW, Young GJ, Alverson AJ, Palmer JD. 2013. The "fossilized"
904   mitochondrial genome of *Liriodendron tulipifera*: ancestral gene content and order,
905   ancestral editing sites, and extraordinarily low mutation rate. *BMC Biology* **11**:1-17.
906   Rico Y, Becerril BAG. 2019. Species delimitation and genetic structure of two endemic
907   Magnolia species (section *Magnolia*; Magnoliaceae) in Mexico. *Genetica*, **147**: 57-68.
908   Rivers MC, Beech E, Murphy L, Oldfield SF. 2016. The Red List of Magnoliaceae-revised and
909   extended. BGCI, Richmond UK. ISBN: 1-905164-64-5
910   Rodríguez-Ramírez EC, Valdez-Nieto JA, Vázquez-García JA, Dieringer G, Luna-Vega I. 2020.
911   Plastic Responses of *Magnolia schiedeana* Schltdl., a Relict-Endangered Mexican Cloud
912   Forest Tree, to Climatic Events: Evidences from Leaf Venation and Wood Vessel Anatomy.

913   *Forests* **11**:737

914 Rozas J, Ferrer-Mata A, Sánchez-DelBarrio JC, Guirao-Rico S, Librado P, Ramos-Onsins SE,
915   Sánchez-Gracia A. 2017. DnaSP 6: DNA Sequence Polymorphism Analysis of Large
916   Datasets. *Molecular Biology and Evolution* **34**:3299-3302.

917 Ruiz-Sánchez E, Ornelas JF. 2014. Phylogeography of *Liquidambar styraciflua* A ltingiaceae in
918   Mesoamerica: survivors of a Neogene widespread temperate forest or cloud forest in
919   North America?. *Ecology and Evolution* **4**:311-328.

920 Rzedowski J. 1978. Vegetación de México. Ed. Limusa, Mexico, DF.

921 Rzedowski J. 1996. Análisis preliminar de la flora vascular de los bosques mesófilos de montaña
922   de México. *Acta Botanica Mexicana* **35**:25–44.

923 Salces-Castellano A, Stankowski S, Arribas P, Patiño J, Karger DN, Butlin R, Emerson BC.
924   2021. Long-term cloud forest response to climate warming revealed by insect speciation
925   history. *Evolution* **75:** 231-244.

926 Sánchez-González LA, Morrone JJ, Navarro-Sigüenza AG. 2008. Distributional patterns of the
927   Neotropical humid montane forest avifaunas. *Biological Journal of the Linnean Society*
928   **94**:175-194.

929 Scoble J, Lowe AJ. 2010. A case for incorporating phylogeography and landscape genetics into
930   species distribution modeling approaches to improve climate adaptation and conservation
931   planning. *Diversity and Distributions* **16**:343-353.

932 SEMARNAT Secretaría de Medio Ambiente y Recursos Naturales. 2010. NOM-059-
933   SEMARNAT-2010 de protección ambiental—especies nativas de México de flora y
934   fauna silvestres—categorías de riesgo, especificaciones para su inclusión, exclusión o
935   cambio lista de especies en riesgo. Diario Oficial de la Federación. 30 de Diciembre del
936   2010. Segunda sección, México.

937 Setsuko S, Tomaru N. 2009. Estimation of outcrossing rates at hierarchical levels of fruits,
938   individuals, populations and species in *Magnolia stellata*. *Heredity* **102**:381-8

939 Shaw J, Lickey EB, Beck JT, Farmer SB, Liu W, Miller J, Siripun KC, Winder CT, Schilling EE,
940   Small RL. 2005. The tortoise and the hare II: relative utility of 21noncoding chloroplast
941   DNA sequences for phylogenetic analysis. *American Journal of Botany* **92**:142–166.

942 Tajima F. 1989. Statistical-method for testing the neutral mutation hypothesis by DNA
943   polymorphism. *Genetics* **123**:585–595.

944 Tobe JD, Abbott AG, Ballard R. 1993. Inheritance of chloroplast DNA in Magnolia. *Magnolia*,
945   **54**:25-31.

946 Toledo VM. 1982. Pleistocene changes of vegetation in tropical Mexico. In G. T. Prance editor,
947   Biological Diversification in the Tropics. Columbia Univ. Press, New York.

948 Toledo-Aceves T, Meave JA, González-Espinoza M, Ramírez-Marcial N. 2011. Tropical
949   montane cloud forest: Current threats and opportunities for the conservation and sustainable
950   management in Mexico. *Journal of Environmental Management* **92**:974-981.

951   Twyford AD, Kidner CA, Harrison N, Ennos RA. 2012. Population history and seed dispersal in
952   widespread Central American *Begonia* species Begoniaceae inferred from plastome-
953   derived microsatellite markers. Botanical Journal of the Linnean Society. **171**:260-76.
954   Vaidya G, Lohman DJ, Meier R. 2011. SequenceMatrix: concatenation software for the fast
955   assembly of multi-gene datasets with character set and codon information. *Cladistics*
956   **27**:171–180.
957   Vásquez-Morales SG, Sánchez-Velásquez LR, del Rosario Pineda-López M, Díaz-Fleischer F,
958   Flores-Estévez N, Viveros-Viveros H. 2017. Moderate anthropogenic disturbance does
959   not affect the demography of *Magnolia schiedeana*, an endangered species from Mexico.
960   *Flora* **234**:77–83.
961   Vásquez-Morales SG, Sánchez-Velásquez LR. 2011. Seed ecology and pre-germinative
962   treatments in Magnolia schiedeana Schlecht, an endangered species from Mexico.
963   *Journal of Food, Ecology and Agriculture* **9**: 604-608.
964   Vásquez-Morales SG, Téllez-Valdés O, del Rosario Pineda-López M, Sánchez-Velásquez LR,
965   Flores-Estevez N, Viveros-Viveros H. 2014. Effect of climate change on the distribution
966   of *Magnolia schiedeana*: a threatened species. *Botanical Sciences* **92:**575–585.
967   Vázquez-García JA, Muñiz-Castro MA, Arroyo F, Pérez AI, Serna M, Cuevas-Guzmán R,
968   Domínguez-Yescas R, de Castro-Arce E, Gurrola-Diaz CM 2013 Novelties of the
969   neotropical *Magnolia* and addendum proposal the IUCN red list of Magnoliaceae. In:
970   Salcedo-Pérez E, Hernández-Álvarez E, Vázquez-García JA, Escoto-García T, Díaz-
971   Echavarría N eds Recursos Forestales en el Occidente de Mexico, Diversidad, Manejo,
972   Aprovechamiento y Conservación. Universidad de Guadalajara. ISBN978-607-8072-73-6
973   Vázquez-García JA, Muñiz-Castro MA, De Castro-Arce E, Murguía R, Nuño A, Cházaro-
974   Basáñez M. 2012. Twenty new Neotropical tree species of *Magnolia. Recursos forestales*
975   *en el occidente de México* **4**:91-130.
976   Vázquez-García JA, Pérez-Farrera MÁ, Gómez-Domínguez H, Muñiz-Castro MA, Sagahún-
977   Domínguez E. 2017 *Magnolia montebelloensis,* a new species in section *Magnolia* from
978   Lagunas de Montebello National Park, Chiapas, México, with a key to Magnoliaceae of
979   Chiapas. *Phytotaxa* **328**:101-114.
980   Vázquez-García JA. 1994. *Magnolia* Magnoliaceae in Mexico and Central America: a synopsis.
981   *Brittonia* **46**:1-23.
982   Venkatraman, MX, Deraad DA, Tsai WLE, Zarza E, Zellmer AJ, Maley JM, McCormack JE.
983   2019. Cloudy with a chance of speciation: Integrative taxonomy reveals extraordinary
984   divergence within a Mesoamerican cloud forest bird. *Biological Journal of the Linnean*
985   *Society* **126**:1–15.
986   Vite A. 2016. Estructura poblacional de *Magnolia schiedeana* Schltdl. en dos ambientes
987   contrastantes en el estado de Hidalgo, México Tesis de maestría. Universidad Autónoma del
988   Estado de Hidalgo, Pachuca, México.
989   Wang YB, Liu BB, Nie ZL, Chen HF, Chen FJ, Figlar RB, Wen J. 2020. Major clades and a
990   revised classification of *Magnolia* and Magnoliaceae based on whole plastid genome

991   sequences via genome skimming. *Journal of Systematics and Evolution* **58:**673– 695.

992   Warren DL, Glor RE, Turelli M. 2008. Environmental niche equivalency versus conservatism:

993   quantitative approaches to niche evolution. *Evolution* **62**:2868-2883.

994   Watanabe K, Ikegami F, Horie S. 2002. Introduction the genus *Magnolia*. In: Satyajit, S.D., Yuji,

995   M. Eds., *Magnolia*: The genus *Magnolia*. Taylor and Francis, New York, USA, pp. 1-7.

996   Wolfe KH, Li WH, Sharp PM. 1987. Rates of nucleotide substitution vary greatly among plant

997   mitochondrial, chloroplast, and nuclear DNAs. *Proceedings of the National Academy of*

998   *Sciences of the United States of America* **84:**9054–9058.

999

1000

Sampling locations, population code, state, species, sample size (n), haplotypes, nucleotide, and haplotype diversity of *M. pedrazae, M. schiedeana* and *M. schiedeana* pop. Oaxaca.

Haplotypes denoted in bold are private haplotypes to the population. State abbreviations as follows: SLP San Luis Potosí, QRO Querétaro, HGO Hidalgo, PUE Puebla, VER Veracruz, OAX Oaxaca

Location	Code	State	Species	n	Haplotypes (no. of individuals)	Nucleotide diversity (π)	haplotype diversity (Hd)
Las Flores	FO	SLP	*M. pedrazae*	3	H18(1), H20(1), **H21**(1)	0.00047	1 ± 0.27
La Silleta	SI	SLP	*M. pedrazae*	4	H31(2), **H46**(1), **H47**(1)	0.00093	0.83 ± 0.2
Coronel Castillo	CS	SLP	*M. pedrazae*	4	H01(1), H02(1), H18(1), **H19**(1)	0.00169	1 ± 0.18
Joya del Hielo & Yesca	JH	QRO	*M. pedrazae*	6	H18(1), H20(1), **H29**(1), **H30**(1), H31(1), **H32**(1)	0.00075	1 ± 0.09
Tlanchinol	TL	HGO	*M. schiedeana*	5	H02(2), H12(1), H35(1), **H48**(1)	0.00105	0.9 ± 0.16
La Mojonera	MO	HGO	*M. schiedeana*	7	H03(2), H25(1), H26(1), H35(2), **H38**(1)	0.00067	0.9 ± 0.1
El Hayal	HA	HGO	*M. schiedeana*	6	H03(3), H26(1), **H27**(1), **H28**(1)	0.00077	0.8 ± 0.17
Tutotepec	TU	HGO	*M. schiedeana*	6	H03(4), H12(1), **H49**(1)	0.00023	0.6 ± 0.2
Medio Monte	MM	HGO	*M. schiedeana*	6	H02(1), H03(1), H15(1), H25(1), H35(1), **H37**(1)	0.0007	1 ± 0.09
El Gosco	GO	HGO	*M. schiedeana*	6	H02(2), H03(1), H15(1), **H24**(1), H25(1)	0.00068	0.93 ± 0.12
El Cirio	CI	HGO	*M. schiedeana*	6	H03(2), **H11**(2), H12(1), **H13**(1)	0.001	0.87 ± 0.13
Tlatlauquitepec	TLA	PUE	*M. schiedeana*	1	**H10**(1)	-	-
Misantla	MI	VER	*M. schiedeana*	1	**H36**(1)	-	-
Volcán de Acatlán	AC	VER	*M. schiedeana*	9	H01(1), H02(1), H03(1), **H04**(1), **H05**(1), **H06**(1), **H07**(1), **H08**(1), **H09**(1)	0.00134	1 ± 0.05
La Martinica	MA	VER	*M. schiedeana*	5	H03(1), H12(1), **H33**(1), **H34**(1), H35(1)	0.00133	1 ± 0.13
Mesa de la Yerba	MY	VER	*M. schiedeana*	5	H03(1), **H39**(1), **H40**(1), **H41**(1), **H42**(1)	0.00154	1 ± 0.13
Cinco Palos	CP	VER	*M. schiedeana*	4	**H14**(1), H15(1), **H16**(1), **H17**(1)	0.00128	1 ± 0.18
Reserva Ecológica	FXC	VER	*M. schiedeana*	2	**H22**(1), **H23**(1)	0.00035	1 ± 0.5
El Zapotal	ZA	VER	*M. schiedeana*	5	H02(1), H03(2), H12(1), H35(1)	0.00042	0.9 ± 0.16
Santiago Comaltepec	SC	OAX	*M. schiedeana* pop Oaxaca	5	**H43**(3), **H44**(1), **H45**(1)	0.0007	0.7 ± 0.22

AMOVA results of distinct hierarchical groups for 20 populations of *M. pedrazae*, *M. schiedeana*, and *M. schiedeana* pop. Oaxaca

Analyzed groups: 1) No predefined groups, 2) populations grouped in two lineages *M. schiedeana* + *M. pedrazae* and *M. schiedeana* pop. Oaxaca and 3) populations grouped by the three lineages corresponding *M. schiedeana*, *M. pedrazae* and *M. schiedeana* pop. Oaxaca. **$P < 0.01$; ***$P < 0.001$.

Grouping	df	Sum of squares	Estimated variance	%	Fixation indices
1. No groups defined					
Among populations	17	78.675	0.6314	32.46	
Within populations	77	101.147	1.3136	67.54	$F_{ST}= 0.325^{***}$
Total	94	179.82	1.945		
2. Two lineages					
Among groups	1	25.126	2.3079	57.58	$F_{CT}= 0.576^{***}$
Among populations within groups	16	53.549	0.3864	9.64	$F_{SC}= 0.227^{***}$
Within populations	77	101.147	1.3136	32.78	$F_{ST}= 0.672^{***}$
Total	94	179.823	4.008		
3. Three lineages					
Among groups	2	50.706	1.3217	48.25	$F_{CT}= 0.483^{***}$
Among populations within groups	15	27.97	0.1041	3.8	$F_{SC}= 0.073^{**}$
Within populations	77	101.147	1.3136	47.95	$F_{ST}= 0.5205^{***}$
Total	94	179.823	2.739		

Genetic diversity, neutrality tests and mismatch distributions for *M. pedrazae*, *M. schiedeana* and *M. schiedeana* pop. Oaxaca.

N number of individuals, N_H number of haplotypes, π nucleotide diversity, H_d haplotypic diversity, D_T Tajima's D, F_S Fu's Fs, *R2* Ramos-Onsins and Rozas, SDD differences in the sum of squares, Hri Harpending´s raggedness index. *$P < 0.05$; **$P < 0.01$

Lineages	N	N_H	π	H_d	D_T	Fs	$R2$	SSD	Hri
M. pedrazae	17	12	0.00098	0.949	-0.524	-0.386	0.117	0.0036	0.0258
M. schiedeana	74	36	0.001	0.923	**-2.09***	**-4.621****	**0.0356****	0.0009	0.0236
M. schiedeana pop. Oaxaca	5	3	0.0007	0.7	-1.12	-1.124	0.253	0.0939	0.290

Figure 1

Sampled localities of *M. pedrazae*, *M. schiedeana* and *M. schiedeana* pop. Oaxaca across the TMCF in Mexico.

State abbreviations see in Table 1.
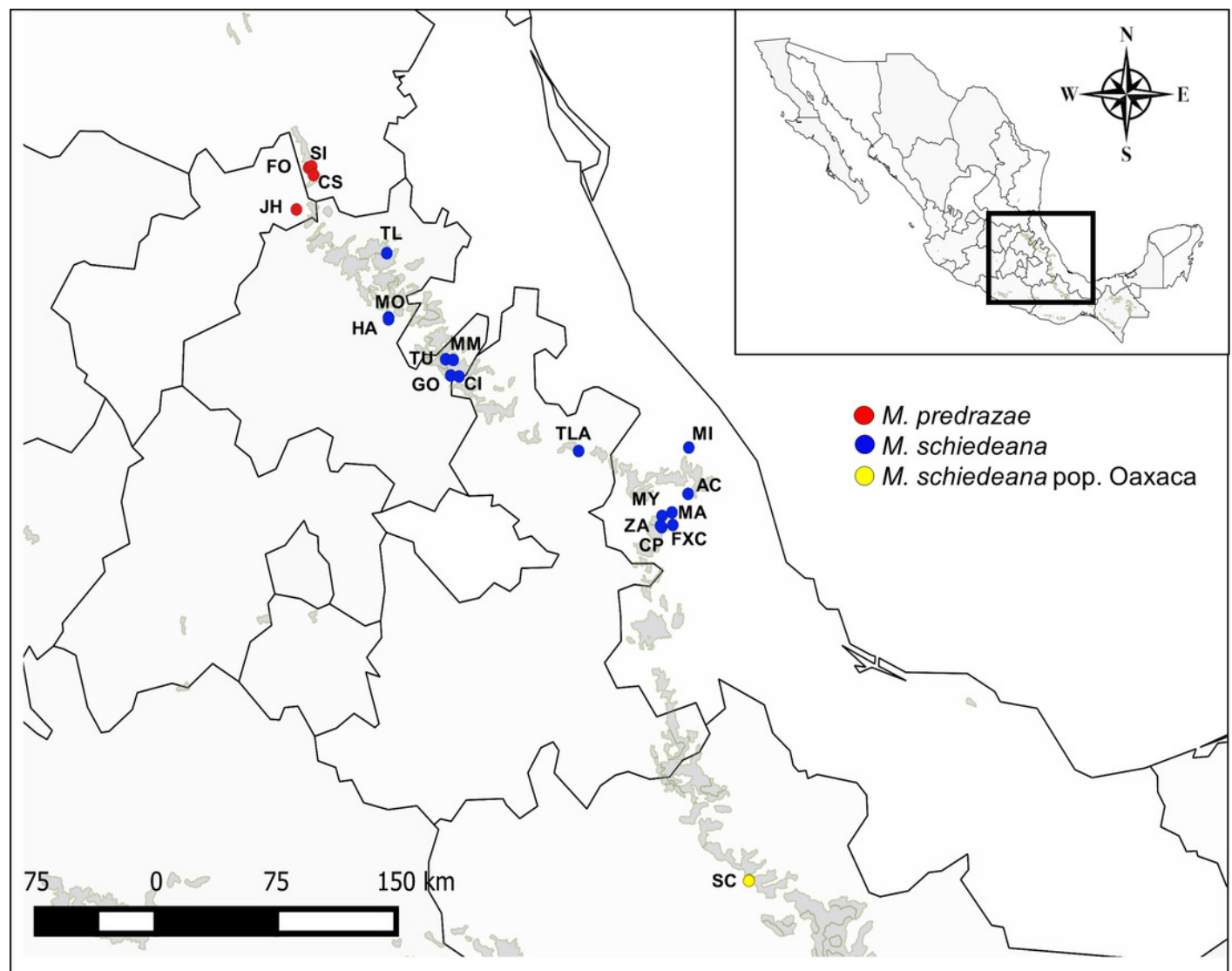
Figure 2

Phylogenetic and haplotype relationships among *M. pedrazae*, *M. schiedeana* and *M. schiedeana* pop. Oaxaca using four concatenated cpDNA regions.

(A) Bayesian phylogenetic tree, (B) Median-joining haplotype network, (C) BAPS *K* = 5 genetic clusters, and (D) BEPC K = 3 genetic clusters and (E-F) PCA plots for eight bioclimatic variables showing the environmental differences for the three clusters. State abbreviations see in Table 1.
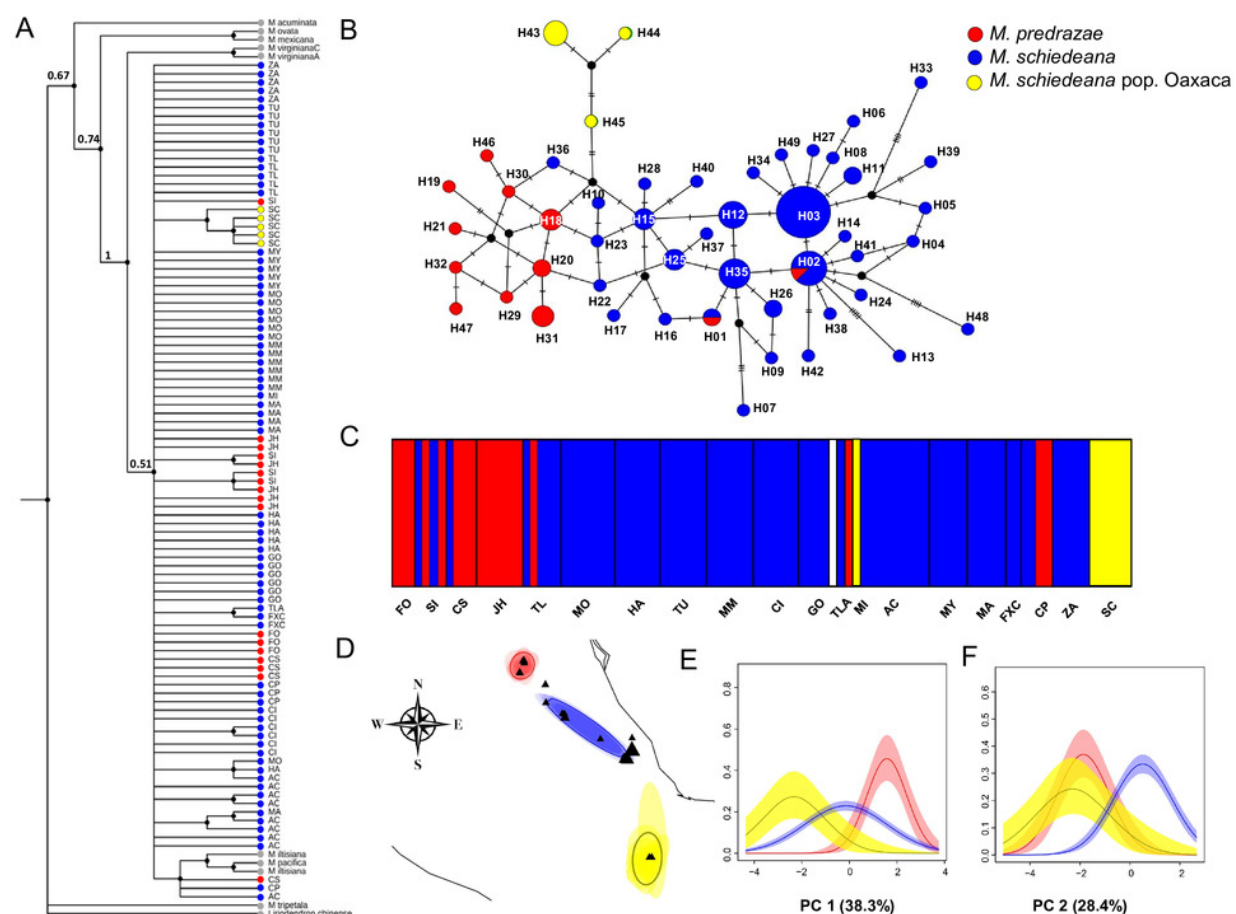
Figure 3

Historical demographic analysis for *M. pedrazae* and *M. schiedeana.*

Mismatch distributions for a sudden expansion model in (A) *M. pedrazae* and (B) *M. schiedeana.* Bayesian skyline plots for (C) *M. pedrazae* and (D) *M. schiedeana.* The blue line traces the inferred median effective population size over time with 95% HPD shaded in blue. The black vertical line is the median projected on the expansion timeline.
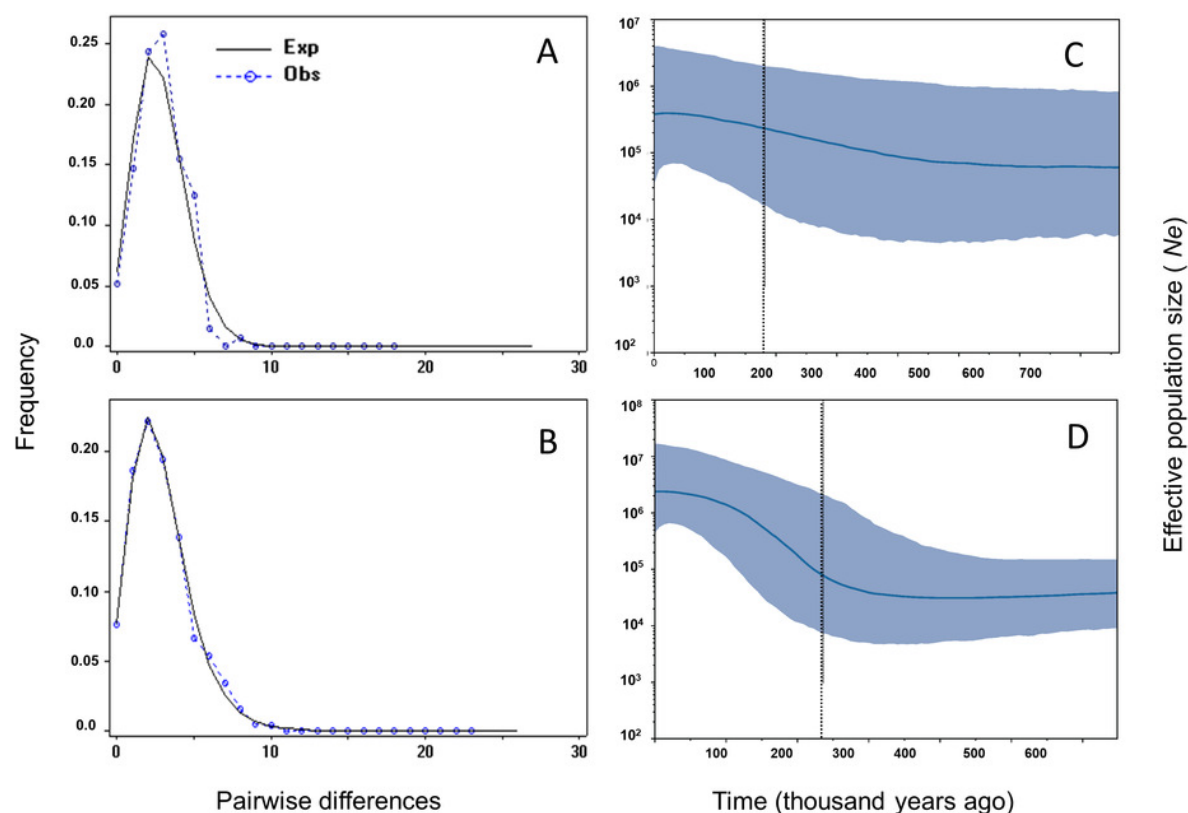
Figure 4

Approximate Bayesian Computation of five competing demographic scenarios for *M. pedrazae*, *M. schiedeana* and *M. schiedeana* pop. Oaxaca simulated in DIYABC

(A) Scenario 1 predicts the three lineages diverging at the same time from a common ancestor (NA) at t_2 (stable model); (B) Scenario 2 predicts a split between *M. schiedeana* and *M. pedrazae* at time t_1, then both merged with *M. schiedeana* pop. Oaxaca at time t_2; (C) Scenario 3 predicts a split between *M. schiedeana* pop. Oaxaca and *M. pedrazae* at t_1 and subsequently both merged with *M. schiedeana* at t_2; (D) Scenario 4 predicts a split between *M. schiedeana* and *M. schiedeana* pop. Oaxaca at t_1 then both merged with *M. pedrazae* at t_2. These three scenarios correspond to a divergence model. (E) Scenario 5 predicts secondary contact between the three lineages at time t_1 (admixture model)
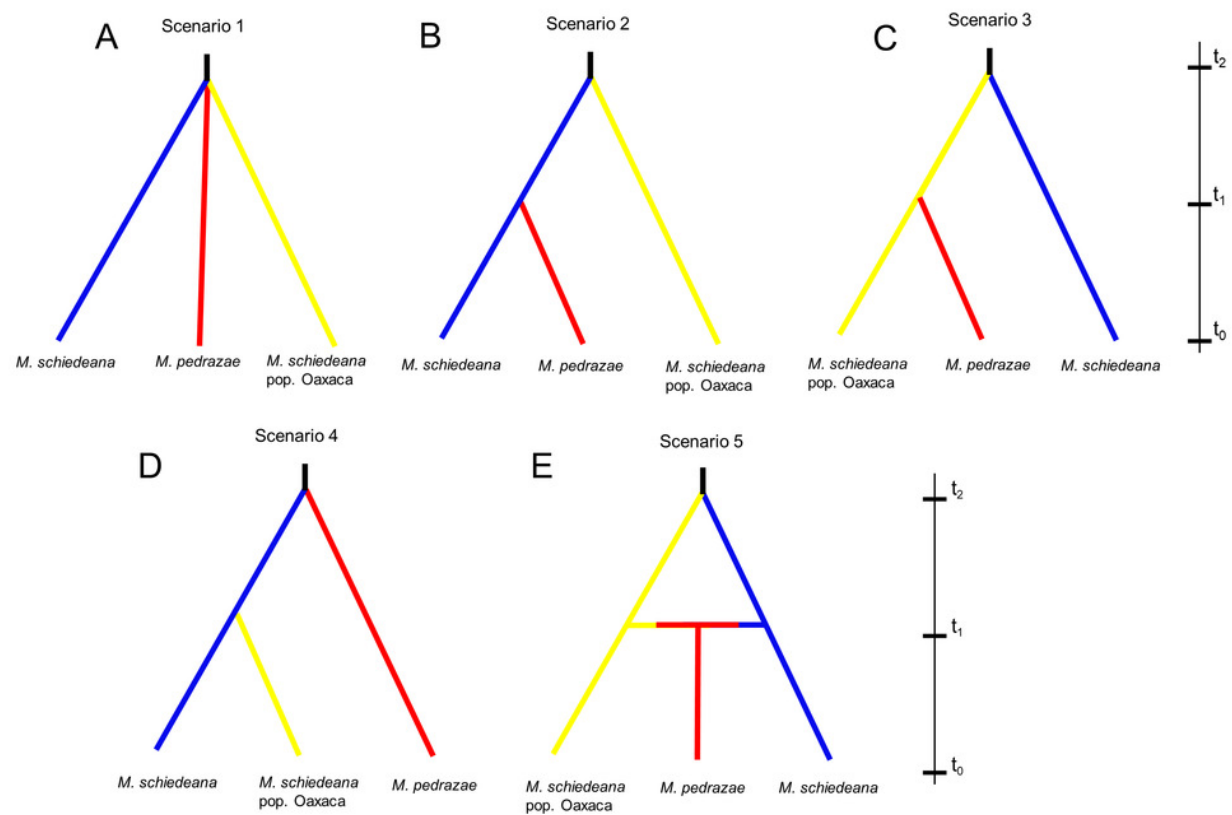
Figure 5

Present and past species distributions modeling for *Magnolia pedrazae* (red dots), *M. schiedeana* (blue dots) and *M. schiedeana* pop. Oaxaca (yellow dots).

A) The three lineage occurrences, (B) Present niche model, (C) Mid-Holocene (MH ~ 8.3 ka), (D) Early Holocene (EH ~ 11.7 ka), (E) Last Glacial Maximum (LGM ~ 23 ka), Last Interglacial (LIG ~ 120 ka).